

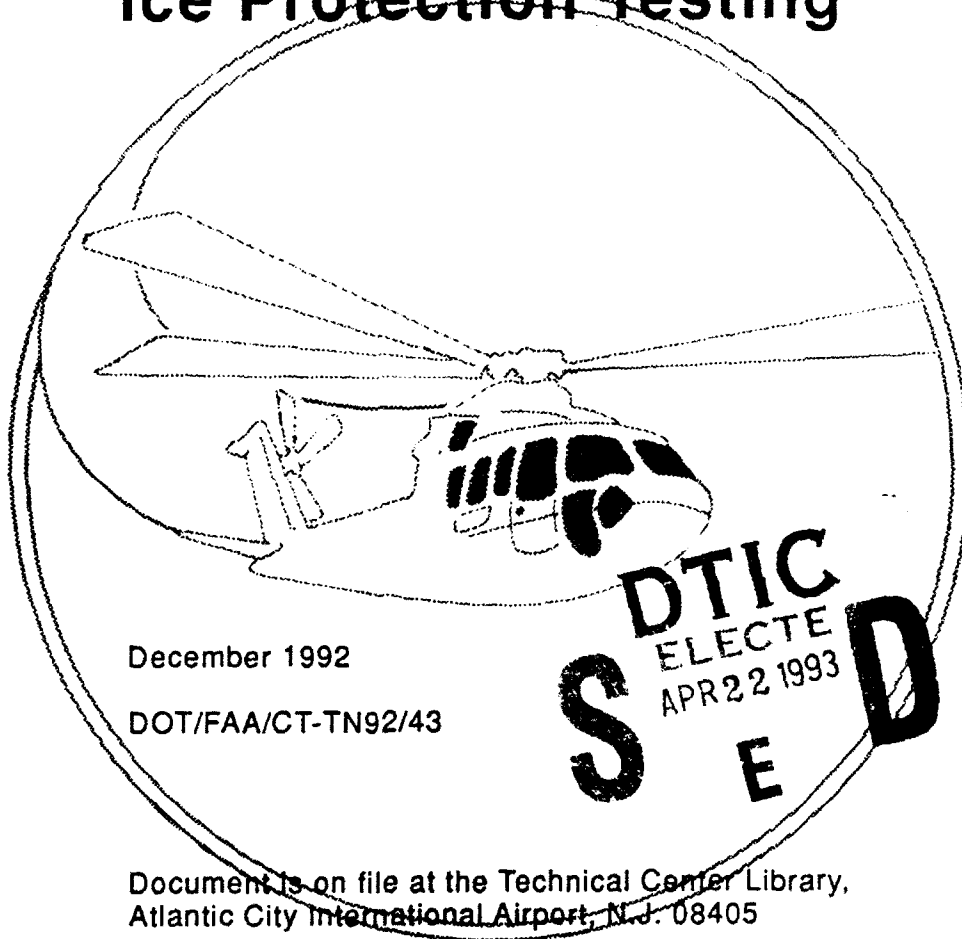
nte technical note technn

AD-A263 203



(2)

Icing Cloud Simulator
for Use In Helicopter Engine
Induction System
Ice Protection Testing



Document is on file at the Technical Center Library,
Atlantic City International Airport, N.J. 08405

4 21 064

93-08616



U.S. Department of Transportation
Federal Aviation Administration

Technical Center
Atlantic City International Airport, N.J. 08405

~~STRIKED OUT STATEMENT~~
Approved for public release
Distribution Unlimited

53Pf

NOTICE

This document is disseminated under the sponsorship of the U. S. Department of Transportation in the interest of information exchange. The United States Government assumes no liability for the contents or use thereof.

The United States Government does not endorse products or manufacturers. Trade or manufacturers' names appear herein solely because they are considered essential to the objective of this report.

Technical Report Documentation Page

1. Report No. DOT/FAA/CT-TN92/43	2. Government Accession No.	3. Recipient's Catalog No.	
4. Title and Subtitle ICING CLOUD SIMULATOR FOR USE IN HELICOPTER ENGINE INDUCTION SYSTEM ICE PROTECTION TESTING		5. Report Date December 1992	
6. Performing Organization Code		7. Author(s) S.W. Brunnenkant	
8. Performing Organization Report No. DOT/FAA/CT-TN92/43		9. Performing Organization Name and Address Heli-Air, Inc. 119 Ida Road Broussard, LA	
10. Work Unit No. (TRAIS)		11. Contract or Grant No.	
12. Sponsoring Agency Name and Address U.S. Department of Transportation Federal Aviation Administration Technical Center Atlantic City International Airport, NJ 08405		13. Type of Report and Period Covered Technical Note	
14. Sponsoring Agency Code ACD-230		15. Supplementary Notes Technical Center Program Manager: Charles Masters	
16. Abstract Aircraft with Airborne Icing Spraying Systems (AISS) have been used for some time to generate icing clouds into which test aircraft could be flown to show compliance with the requirements of FAR XX.1093. However, the spray arrays used and the relatively large distance between the AISS and aircraft parts to be tested precluded small droplet sizes at high liquid water content at most atmospheric conditions. Some of these shortcomings were overcome by mounting the AISS directly on the test aircraft. This proved to be a very efficient method to develop and certify individual aircraft components. This report describes the methodology and test procedure used with an AISS mounted on a test aircraft to show compliance with FAR 29.1093 for the newly developed inlet of the Bell 222/250-C30G helicopter conversion. Development and certification testing was accomplished in a 4-week period.			
17. Key Words Aircraft Ice Protection Airborne Icing Spraying System AISS Icing, Inlet		18. Distribution Statement Document is on file at the Technical Center Library, Atlantic City International Airport, New Jersey 08405	
19. Security Classif. (of this report) Unclassified	20. Security Classif. (of this page) Unclassified	21. No. of Pages 50	22. Price

PREFACE

The test equipment described in this report was designed and built for and by Heli-Air, Inc. of Broussard, LA. Flight tests were conducted in International Falls, Minnesota and Ames, Iowa. Tyron Millard and Wayne Barbini represented the Rotorcraft Directorate of the Southwest Region of the Federal Aviation Administration (FAA). Harry Harr, designated engineering representative of Global Helicopters, coordinated Heli-Air's efforts with the FAA and recorded aircraft parameters and liquid water content during testing. Dave Brown of Heli-Air, Inc., piloted the aircraft. Paul Graham and John Eastes (Heli-Air), under the direction of Dave Brown, kept the helicopter flying as well as provided video and still picture coverage of the tests in progress. The author operated the spray rig and photographed the icing cloud droplet samples captured on oil slides. The aircraft tested was a modified Bell 222A helicopter.

Accesion For	
NTIS	CRA&I <input checked="" type="checkbox"/>
DTIC	TAB <input type="checkbox"/>
Unannounced	<input type="checkbox"/>
Justification	
By	
Distribution /	
Availability Codes	
Dist	Avail and/or Special
A-1	

DTIC QUALITY INSPECTED

TABLE OF CONTENTS

	Page
EXECUTIVE SUMMARY	xi
1. INTRODUCTION	1
2. DISCUSSION	1
2.1 Bleed Air	1
2.2 Spray Nozzle	2
2.3 Droplet Impingement Temperature	2
2.4 Impact Velocity	3
2.5 Spray Rig Design and Controls	4
3. AIRCRAFT CONFIGURATION AND TEST SETUP	5
3.1 Induction System	5
3.2 Test Setup	5
4. TEST CONDITIONS	6
5. DATA ACQUISITION	7
6. RESULTS OF TESTING	8
6.1 Introduction	8
6.2 Summary of Testing Conclusions	8
6.3 Operational Notes	8
6.4 Droplet Quality	11
6.5 Temperature	12
6.6 Inlet Performance	12
7. CONCLUSIONS/OBSERVATIONS	12
8. REFERENCES	16

LIST OF FIGURES

Figure	Page
1 Available Bleed Air per Engine at 60 KIAS (4.2% Bleed, Std Day)	17
2 Spray Nozzle	18
3 Spray Nozzle Performance	19
4 Code to Calculate Droplet Impact Conditions (3 sheets)	20
5 Droplet Trajectory Calculations, MVD = 25 μm	22
6 Droplet Trajectory Calculations, MVD = 45 μm	24
7 Design Code for Ice Rig	25
8 Typical Output from Design Code (Figure 7)	26
9 Spray Rake Configuration	27
10 Nozzle Feed Details	28
11 Test Equipment Schematic	29
12 Test Aircraft Configuration and Setup (Schematic)	30
13 Inlet Screens	31
14 Test Aircraft Configuration Photos (Spray Rig)	32
15 Test Aircraft Configuration Photos (Engine Inlet)	33
16 Actual Rake Performance	34
17 Droplet Size Distribution	35
18 RUN 5A, Maximum Inlet Ice Buildup MVD = 26, KIAS = 50, OAT = 17°F	36
19 RUN 5B, Maximum Inlet Ice Buildup MVD = 26, KIAS = 100, OAT = 15°F	36
20 RUN 5C, Maximum Inlet Ice Buildup MVD = 21, KIAS = 75, OAT = 16°F	37
21 RUN 5D, Maximum Inlet Ice Buildup MVD = 40, KIAS = 100, OAT = 19°F	37

LIST OF ILLUSTRATIONS (Continued)

Figure		Page
22	RUN 5E, Maximum Inlet Ice Buildup MVD = 58, KIAS = 50, OAT = 17°F	38
23	RUN 6A, Maximum Inlet Ice Buildup MVD = 26, KIAS = 50, OAT = 11°F	39
24	RUN 6B, Maximum Inlet Ice Buildup MVD = 25, KIAS = 50, OAT = 14°F	39
25	RUN 7A, Maximum Inlet Ice Buildup MVD = 18, KIAS = 50, OAT = -4°F	40
26	RUN 7B, Maximum Inlet Ice Buildup MVD = 25, KIAS = 100, OAT = -2°F	41
27	RUN 8A, Maximum Inlet Ice Buildup MVD = 43, GROUND RUN, OAT = 24°F	41
28	RUN 9A, Maximum Inlet Ice Buildup MVD = N.A., GROUND RUN, OAT = 32°F	42
29	RUN 9B, Maximum Inlet Ice Buildup MVD = 42, KIAS = 50, OAT = 31°F	42

LIST OF TABLES

Table		Page
1	Proposed Test Conditions	9
2	Actual Test Conditions Flown	9
3	Bell 222/250-C30G Ice Test Result	10
4	Bell 222/250-C30G Ice Buildup. Test Results Summary (2 sheets)	13
5	Bell 222/Allison 250-C30G Inlet Losses due to Icing	15

SYMBOLS AND ABBREVIATIONS

A_{A_2}	- Air Exit Area into Nozzle Mixing Chamber
A_{A_3}	- Net Effective Nozzle Exit Area for Air
A_3	- Nozzle Exit Area
A_c	- Icing Cloud Area
A_{W_2}	- Water Exit Area into Nozzle Mixing Chamber
C_D	- Water Droplet Drag Coefficient
C_v	- Discharge Coefficient
D_w	- Water Droplet Diameter
dV/dt	- Rate of Change of Water Droplet Velocity
FAA	- Federal Aviation Administration
FAR	- Federal Aviation Regulation
FOD	- Foreign Object Damage
g	- Gravitational Constant
GPH	- Gallons Per Hour
h_c	- Heat Transfer Coefficient
IFR	- Instrument Flight Rules
k	- Specific Heat Ratio
KIAS	- Knots Indicated Air Speed
LWC	- Liquid Water Content
MVD	- Mean Volume Diameter
N	- Number of Steps to Calculate Jet Core Velocity and Temperature
N_u	- Nusselt Number
OAT	- Outside Air Temperature
P_{A_1}	- Nozzle Air Supply Pressure
P_2	- Mixing Chamber Pressure
P_{W_1}	- Nozzle Water Supply Pressure

P_R	- Prandtl Number
R_C	- Temperature Recovery Factor
R_g	- Gas Constant for Air
R_N	- Reynolds Number
T_∞	- Remote Air Temperature
T_{A_1}	- Nozzle Supply Air Temperature
T_{A_2}	- Mixing Chamber Air Temperature (Isentropic)
T_{A_2}'	- Mixing Chamber Air Temperature (Actual)
T_{A_J}	- Jet Core Air Temperature
T_{OT}	- Turbine Outlet Temperature
T_{W_J}	- Jet Core Water Droplet Temperature
V_{A_J}	- Jet Core Velocity of Air
V_{A_2}	- Air Velocity Into Mixing Chamber
V_∞	- Remote Air Velocity (Aircraft)
V_R	- Relative Velocity between Water Droplet and Jet Core Air Velocity
V_{W_J}	- Water Droplet Velocity in Jet Core
W_A	- Airflow Rate through Nozzle
w_A	- Specific Weight of Air
w_W	- Specific Weight of Water
X	- Distance Along Jet Core Measured Downstream of Nozzle Exit

EXECUTIVE SUMMARY

Airborne Icing Spray Systems (AISS) have proved to be valuable tools in the development and certification process of complete aircraft as well as aircraft components. This report details the design methodology and test procedure of an AISS mounted directly on the test aircraft. The system was used to develop and show compliance with the requirements of Federal Aviation Regulations (FAR) 29.1093 for a new engine inlet on the Bell 222/250-C30G helicopter conversion.

This AISS design entailed investigation of available bleed air and water supplies, spray nozzle performance in terms of required water and bleed air quantities, pressures and temperatures to generate the desired droplet sizes, droplet size distribution, droplet impact temperature and velocities, icing cloud freezable liquid water content, etc., all for various atmospheric conditions and airspeeds. Computer code was generated to facilitate the design process.

It was found that the entire FAR Part 29, Appendix C envelope could be simulated with the nozzle arrangement and systems controls provided. The entire development and certification testing was accomplished within a 4-week period. This was due to the fact that the system was self-sufficient and therefore operationally and logistically very flexible.

1. INTRODUCTION.

In early 1988, the design process of replacing the two LTS-101 engines in the Bell 222 helicopter with Allison 250-C30G engines was initiated by Heli-Air, Inc. of Louisiana. Due to the different air inlet configuration of these engines, the air induction system had to be redesigned. Part of the Supplemental Type Certificate (STC) work was, therefore, to show compliance with the requirements of Federal Aviation Regulation (FAR) Part 29, paragraph 1093, dealing with induction system ice protection. Due to a tight schedule and budgetary considerations, it was decided to avoid, if possible, icing tunnel schedules and/or the high costs of currently used ground or airborne icing cloud generators.

Previous experience by the author with small arrays of spray nozzles used on the ground in appropriate weather conditions had been shown to perform in a satisfactory manner for small turboprop air induction systems. However, this could not be said of a similar setup used on a helicopter. Rotor wash and lack of a sufficient horizontal wind-component made it difficult to control the icing cloud produced, let alone simulate forward airspeed. It was therefore concluded that for this case a cost effective and workable icing rig should be airborne, necessarily self-sufficient, and mounted on the aircraft whose air induction system was to be tested.

This report describes the design process for such a spray rig, as well as results obtained using this system. The nozzle array considered was to be sized to adequately cover the starboard engine inlet with an icing cloud sufficiently variable to cover atmospheric icing as detailed in FAR Part 29, Appendix C. The following items were considered before the spray rig configuration was finalized:

1. Sufficiency of available bleed air in terms of volume, temperature, and pressure.
2. Nozzle performance and control requirements.
3. Droplet impingement temperatures and velocity.

2. DISCUSSION.

2.1 BLEED AIR.

The maximum extractable bleed air for the Allison 250-C30G engines is 4.5 percent of the airflow rate. To estimate the minimum amount of bleed air available, power required was assumed to be 235 hp/engine. At this power setting, the Allison 250-C30G engine performance program gives the bleed airflow rates, pressures and temperatures as shown on figure 1.

2.2 SPRAY NOZZLE.

The spray nozzles used were manufactured by the Spraying Systems Company of Wheaton, IL. The particular setup selected (after some bench tests) consisted of fluid cap 40100 and air cap 1401110 (figure 2). At a water flow rate of 2.5 GPH, this internal mix nozzle produced water droplets in the size range required (figure 3). Manufacturer supplied test data was used to relate water pressure, P_{W_1} , air supply pressure, P_{A_1} and water flow rate, GPH, as follows:

$$P_{W_1} = .572 P_{A_1} + 2.56 \text{ GPH} - 7.4$$

The mixing chamber pressure, STA 2, was calculated from:

$$P_2 = P_{W_1} - (.00232 \text{ GPH}/A_{W_1})^2/2 g w_w$$

The compressible flow equation was then used to calculate airflow rates and mixing chamber inlet velocity.

Let $R = (P_2/P_{A_1})$
 $C_1 = (2)(g)(k/k-1)$
 $C_2 = 2/k$
 $C_3 = (k-1)/k$

Then

$$W_A = P_{A_1} C_V A_{A_2} [(C_1/R_g T_{A_1})(R^{C_2})(1-R^{C_3})]^{1/2}$$

And

$$V_{A_2} = [C_1 R_g T_{A_1} (1-R^{C_3})]^{1/2}$$

Based on experimental data, the discharge coefficient, C_V , was determined to be .7. A temperature recovery factor of .9 was assumed.

$$RC = (T_{A_1} - T_{A_2'}) / (T_{A_1} - T_{A_2}) = .9$$

To be on the conservative side as far as target impact temperatures are concerned, the nozzle air exit temperature was assumed to be equal to mixing chamber inlet temperature. The nozzle air exit velocity was based on the net mixing chamber exit area, that is:

$$A_{A_3} = A_3 - A_W$$

2.3 DROPLET IMPINGEMENT TEMPERATURE.

The following assumptions were made regarding the droplet path to the target.

- a. A spray nozzle rake of sufficient size could be mounted about 7 feet ahead of the engine inlet.
- b. The water droplets are spherical.

c. The Reynolds number is low enough such that the droplet drag coefficient is approximated by:

$$C_D = 24 / R_N$$

d. The velocity and temperature decay of the jet core are approximated by:

$$V_{AJ} = (6D_3/X (V_{AJ_3} - V_\infty)) + V_\infty$$

$$T_{AJ} = (5D_3/X (T_{AJ_3} - T_\infty)) + T_\infty$$

To be on the conservative side, jet core parameters have been used to compute target impact conditions.

2.4 IMPACT VELOCITY.

The change in droplet velocity is given by:

$$\begin{aligned} dV/dt &= \text{droplet drag/droplet mass} \\ &= (3/4)(w_A/w_w)(C_D/D_w) V_R \end{aligned}$$

Substituting assumption "C", and assuming the viscosity to be constant over the temperature range in question, this equation reduces to:

$$dV/dt = 18 \mu (V_R / D_w^2)$$

In the interval, delta X, bounded by station 1 and 2, the average relative velocity, V_R , is estimated as follows:

$$V_R = (V_{AJ_1} + V_{AJ_2} - V_{wJ_1} - V_{wJ_2})/2$$

And the corresponding time increment:

$$(t_2 - t_1) = 2 (X_2 - X_1) / (V_{wJ_2} - V_{wJ_1})$$

Where $(X_2 - X_1) = (\text{distance to target})/N$
Combining yields

$$\begin{aligned} 0 &= V_{wJ_2}^2 + 18 \mu (X_2 - X_1) V_{wJ_2} / D_w^2 \\ &\quad - [V_{wJ_1}^2 + 18 \mu (X_2 - X_1) (V_{AJ_1} + V_{AJ_2} - V_{wJ_1}) / D_w^2] \end{aligned}$$

This can now be solved for V_{wJ_2} .

2.4.1 Water Impact Temperature.

For the purpose of this investigation, only worst case conditions are investigated to assure that prescribed icing conditions are satisfied. It was therefore decided that evaporative cooling of the water droplet will be ignored.

The same step size has been used as for the velocity calculations. The initial droplet temperature was assumed to be the water supply temperature (heating in the mixing chamber of the nozzles has been ignored). The droplet temperature exposed to the jet core and airstream is evaluated for each step using the solution to the transient heat transfer equation

$$T_{WJ2} = (T_{WJ1} - T_{AJAV}) e^{-[(H_{cAs})/(w_w V)]t} + T_{AJAV}$$

Where

$$H_c = N_u k / D_w$$

The Nusselt number, N_u , for a sphere, is given by:

$$N_u = 2 + (.4R_N^{1/2} + .06 R_N^{2/3})(P_R)^{.4}$$

The Prandtl number, P_R , for the case on hand was assumed to be .71. Reynolds and Nusselts numbers are based on the diameter of the water droplet.

The computer code on figure 4 has been used to calculate the temperature and velocity of a water droplet traveling along the jet core. Figure 5 gives the characteristics of a 25 μ m particle while figure 6 shows temperatures and velocity of a 45 μ m droplet. The last column in the tabulations shows the differential speed between jet core and water droplet.

As shown, essentially ambient conditions exist 3 to 4 feet past the spray rake, especially if one remembers that the data shown are based on a temperature and velocity decay of a smooth nozzle. The highly turbulent spray nozzle exit conditions should provide a much earlier and more uniform particle stabilization than what this math model indicates.

2.5 SPRAY RIG DESIGN AND CONTROLS.

The total amount of water to generate the appropriate icing cloud is given by:

$$GPH = .045 gr V_w A_c / \sqrt{\delta}$$

The nozzle configuration selected runs best at water flow rates of 2.5 GPH. A curve fit to experimental data (figure 1) yields the air pressure required to operate this nozzle as a function of desired droplet size in microns.

$$P_{A1} = .094 D_w^2 - 6.64 D_w + 132.2$$

The corresponding water pressure to force a flow of 2.5 GPH is given by:

$$P_w = .572 * P_{A1} - 1$$

Using these relationships, computer code was generated (Figure 7) to yield optimum rake configurations for each required condition. For the worst case, the number of nozzles required at 2.5 GPH/nozzle was 30 (see figure 8). To be able to generate all required icing clouds, a spray array of 34 nozzles was devised which allowed the operation of uniformly spaced nozzles in groups of 9, 25, and 34. Figure 9 shows the final rake configuration. Bleed air enters

the vertical distribution trunk (3) at (1) feeding all nozzles. Water enters two separate sets of passages supplying the 9 and 25 nozzles groups [(5) and (4) at (2)]. The shroud (6) helps to dampen rake-caused turbulence as well as to direct the icing cloud. Figure 10 details the distribution system to spray nozzle sets (4) and (5). Water as well as air passages are designed to minimize differences in pressure drops to each nozzle. A schematic of the test equipment setup is shown on figure 11. A metering pump (2) delivers water at a constant flow rate from the 30 gallon water tank (1), via a filter (5), and a flow meter (8) to the spray rig. An accumulator (3) downstream of the pump smoothes out the variable supply pressure. Bleed air pressure and waterflow rates were predetermined and could be preset using metering valve (7) and bypass valve (9) in conjunction with gate valve (2) on the air supply side.

Bleed air was also used to power the LWC meter mounted forward of the engine inlet. Air and water temperatures and pressures were measured at the spray rig. A shock mounted microscope provided a means to determine droplet sizes captured on oil slides during individual runs.

3. AIRCRAFT CONFIGURATION AND TEST SETUP.

The aircraft configuration and test setup is schematically shown on figure 12. Figures 13, 14, and 15 show configuration photos of the test aircraft.

3.1 INDUCTION SYSTEM.

Air enters the inlet plenum (figure 12) through a perforated metal screen (5) and an alternate air passage (6). From there it flows through a coarse FOD screen (7) via a converging duct (8) to the Bellmouth of the Allison 250-C30G engine (10).

During icing conditions, the perforated metal screen (5) acts as a valve by freezing over within seconds and thus forcing all the air to flow through the alternate air passage (6). It is expected that inertial separation of water particles and air will keep the plenum ice free. Although some run through screen (5) freezes over, the amount of internal ice buildup was expected to be minimal. In any case, FOD screen (7) is expected to protect the engines from any ice breaking loose from screen (5) or entering through the air bypass (6) when the rotorcraft reenters nonicing conditions.

3.2 TEST SETUP.

The spray rig (1) was mounted on top of the cabin over the pilot's seat (figure 12). The shroud and flap attached to the top trailing edge of the shroud were made adjustable to allow centering of the icing cloud on the #2 engine inlet screen (5). The liquid water content sensor (2) was mounted near the top of the gearbox cowl. An 8-inch-long, 1/4-inch-diameter rod (3) installed perpendicular to the gearbox ahead of the inlet demonstrated ice accretion rates and ice shapes during testing.

Spray rig pressure and temperatures were measured at the rake's water and bleed air inlets. To monitor the ice cloud's temperature history, thermocouples were located at the trailing edge of the 8-inch rod at (4) and at the FOD screen (7).

OAT was recorded using a thermocouple located within 2 inches of the ship OAT sensor. A single pitot-static tube (9) ahead of the engine bell mouth (10) was used to estimate inlet losses under icing conditions. To sample droplet sizes, an oil slide could be exposed to the icing cloud through a tube in the cabin roof just ahead of the inlet. Mirrors mounted ahead of the spray rig allowed the pilot to observe the location of the icing cloud. A mirror located on the top of the starboard winglet made it possible to film the inlet screen and the 8-inch rod from the cabin while a test was in progress. All spray rig controls were located in the cabin.

4. TEST CONDITIONS.

The Bell Helicopter Model 222 is not certified to fly into known icing conditions. The air induction system certification was therefore based on the concept of limited exposure associated with escape from inadvertent icing encounters.

Since the physical size of the icing clouds to be traversed has been defined, the total amount of ice accretion for a given catch efficiency is a function of the freezing water fraction (LWC) only, whereas the ice accretion rate for a given LWC and catch efficiency in the externals of the inlet is proportional to the ship's airspeed, internal ice buildup in the air induction system is a function of the engines volumetric air consumption. To minimize the effects of the icing conditions, one should therefore fly the helicopter at the low speed end of the drag curve. The less efficient inertial water removal from the combustion air at low forward speeds is expected to be secondary. At higher speeds, screen run through and/or projected higher inlet losses may become critical. For the above reason, the minimum IFR speed of 50 KIAS appears to be a practical initial penetration speed.

Table 1 shows the proposed test conditions and estimates total ice accretion while on condition. Conditions (1)-(5) are flown at just below freezing temperature. Conditions (1) and (2) are flown at max ice accretion rates. Condition (3) checks for potential problems in case of nonrecognition of icing conditions. Seventy-five KIAS is deemed a reasonable average speed for flight in prevailing atmospheric conditions. Conditions (4) and (5) are the worst cases for water flow through on screen #1. Conditions (6) and (7) are run at lower temperatures to show the effects of ice shapes.

5. DATA ACQUISITION.

Flight test data included the following parameters:
Aircraft Data:

OAT - Outside Air Temperature
VI - Indicated Airspeeds
TQ - Torque (both engines)
HP - Altitude (Pressure)
TOT - Turbine Outlet Temperature (both engines)
 N_1 - Compressor Speed
GW - Gross Weight
PSI-PSS - Inlet Static Pressure
PTI-PSS - Inlet Total Pressure
PTS-PSS - Ship Total Pressure

Spray Rig:

LWC - Freezable Liquid Water Content
WFR - Water Flow Rate
TNA - Air Temp (Nozzle Inlet)
PNA - Air Press (Nozzle Inlet)
TNW - Water Temp (Nozzle Inlet)
THS₁ - Icing Wand Temperature (Icing Cloud)
THS₂ - Coarse Screen Temp (Inlet Air Temp)
PNW - Water Press (Nozzle Inlet)

6. RESULTS OF TESTING.

6.1 INTRODUCTION.

Company testing conducted between February 23 and March 13, 1989, confirmed the predicted capabilities of the aircraft mounted, self-contained spray rig. Limited icing tests during this period also established sufficient confidence in the air induction system design to start FAA testing. All testing was done March 13 through 15, 1989, in International Falls, Minnesota, and on March 18 and 19 in Ames, Iowa. FAA representatives of the Rotorcraft Certification Directorate of the Southwest Region witnessed the conduct of the tests.

The aircraft tested was a modified Bell 222A with the following deviations:

- a. LTS-101 engines were replaced with Allison 250-C30G engines.
- b. Different exhaust system.
- c. Different inlet system.
- d. Ice rig mounted on top of forward cabin.

Figures 14 and 15 give an overview of the test aircraft while figure 13 shows the two outer screens ("small" on the left side, "large" on the right side) tested.

Engineering judgement based on early test results dictated changes in the proposed test plan. Table 2 shows actual conditions flown. Table 3 summarizes the raw test data taken during the FAA witnessed test period.

6.2 SUMMARY OF TESTING CONCLUSIONS.

The FAA representatives concurred that based on the observed test results, the air induction system flown will adequately protect the engines from detrimental ice buildup during inadvertent flight into icing conditions. Subsequent analysis of droplet size and LWC's showed that these parameters were essentially within specified limits. The TOT margins were also found to be sufficient. It was, therefore, concluded that the Bell 222A/Allison 250-C30G as configured meets the requirements of FAR Part 29, Appendix C of the CFR's.

6.3 OPERATIONAL NOTES.

All test points were run near maximum gross weight. To maximize bleed air available to the spray rig, all test conditions were flown with the landing gear extended.

The time duration of each test point was determined by the time required to transverse sequentially a standard stratiform and cumuliform cloud as defined in Part 29, Appendix C. Since the Ludlum limit reduces the useful range of the freezable liquid water content meter to 2 gm/m^3 and because cumuliform clouds may reach up to 3 gm/m^3 , the time to simulate these conditions was increased by a factor of 1.5 and the target LWC was reduced to a measurable 2 gm/m^3 . Furthermore, 1 minute was added to allow for a problem recognition time.

	KIAS	OAT F	MVD	LWC	TIME	mm ICE ACRETION
1	50	26-31	15-25	1.8-2.0	5.3	15.9
			15-25	0.5-0.8	21.9	22.0
2	100	26-31	15-25	1.8-2.0	3.2	17.6
			15-25	0.5-0.8	11.4	24.0
3	75	26-31	15-25	0.5-0.8	30.0	42.0
4	50	26-31	35-50	0.5-.75	5.3	5.3
			35-50	.15-.30	21.9	8.8
5	100	26-31	35-50	0.5-.75	3.2	6.2
			35-50	.15-.30	11.4	6.6
6	50	10-15	15-25	1.8-2.0	5.3	15.9
			15-25	0.5-0.8	21.9	22.0
7	100	10-15	15-25	1.8-2.0	3.2	17.6
			15-25	0.5-0.8	11.4	24.0

Table 1. Proposed Test Conditions

COND.	KIAS	OAT	TIME	LWC	MVD
5C	75	16.2	30.0	1.02	21
9B	50	31	22.0	1.77	42
5A	50	16.6	5.3	2.62	19
			21.7	1.28	22
5B	100	14.7	6.4	2.13	28
			12.4	0.71	25
5E	50	16.7	5.3	1.34	58
			21.9		
5D	100	18.7	6.4	0.80	40
			12.4	0.58	41
8A		23.6	40.0	0.88	43
9A		32.0	30.0	2.10	
7A	50	-4	5.3	2.46	19
			21.9	1.08	17
7B	100	-2	6.4	1.74	25
			12.4	0.71	25
6A	50	10.5	27.0	1.94	26
6B	50	14	21.9	1.12	25
			5.3	1.86	25
6D	50	15	21.9	0.90	29
			5.3	2.15	21

Table 2. Actual Test Conditions Flown

 **BELL-AIR**
Subsidiary

RAW DATA

DATE	COLD	WARM	ALT	ELAS	ALT	ELAS	TIME	T05	T15	T25	T35	T45	T55	T65	T75	T85	T95	T105	T115	T125	T135	T145	T155	T165	T175	T185	T195	T205	T215	T225	T235	T245	T255	T265	T275	T285	T295	T305	T315	T325	T335	T345	T355	T365	T375	T385	T395	T405	T415	T425	T435	T445	T455	T465	T475	T485	T495	T505	T515	T525	T535	T545	T555	T565	T575	T585	T595	T605	T615	T625	T635	T645	T655	T665	T675	T685	T695	T705	T715	T725	T735	T745	T755	T765	T775	T785	T795	T805	T815	T825	T835	T845	T855	T865	T875	T885	T895	T905	T915	T925	T935	T945	T955	T965	T975	T985	T995	T1005	T1015	T1025	T1035	T1045	T1055	T1065	T1075	T1085	T1095	T1105	T1115	T1125	T1135	T1145	T1155	T1165	T1175	T1185	T1195	T1205	T1215	T1225	T1235	T1245	T1255	T1265	T1275	T1285	T1295	T1305	T1315	T1325	T1335	T1345	T1355	T1365	T1375	T1385	T1395	T1405	T1415	T1425	T1435	T1445	T1455	T1465	T1475	T1485	T1495	T1505	T1515	T1525	T1535	T1545	T1555	T1565	T1575	T1585	T1595	T1605	T1615	T1625	T1635	T1645	T1655	T1665	T1675	T1685	T1695	T1705	T1715	T1725	T1735	T1745	T1755	T1765	T1775	T1785	T1795	T1805	T1815	T1825	T1835	T1845	T1855	T1865	T1875	T1885	T1895	T1905	T1915	T1925	T1935	T1945	T1955	T1965	T1975	T1985	T1995	T2005	T2015	T2025	T2035	T2045	T2055	T2065	T2075	T2085	T2095	T2105	T2115	T2125	T2135	T2145	T2155	T2165	T2175	T2185	T2195	T2205	T2215	T2225	T2235	T2245	T2255	T2265	T2275	T2285	T2295	T2305	T2315	T2325	T2335	T2345	T2355	T2365	T2375	T2385	T2395	T2405	T2415	T2425	T2435	T2445	T2455	T2465	T2475	T2485	T2495	T2505	T2515	T2525	T2535	T2545	T2555	T2565	T2575	T2585	T2595	T2605	T2615	T2625	T2635	T2645	T2655	T2665	T2675	T2685	T2695	T2705	T2715	T2725	T2735	T2745	T2755	T2765	T2775	T2785	T2795	T2805	T2815	T2825	T2835	T2845	T2855	T2865	T2875	T2885	T2895	T2905	T2915	T2925	T2935	T2945	T2955	T2965	T2975	T2985	T2995	T3005	T3015	T3025	T3035	T3045	T3055	T3065	T3075	T3085	T3095	T3105	T3115	T3125	T3135	T3145	T3155	T3165	T3175	T3185	T3195	T3205	T3215	T3225	T3235	T3245	T3255	T3265	T3275	T3285	T3295	T3305	T3315	T3325	T3335	T3345	T3355	T3365	T3375	T3385	T3395	T3405	T3415	T3425	T3435	T3445	T3455	T3465	T3475	T3485	T3495	T3505	T3515	T3525	T3535	T3545	T3555	T3565	T3575	T3585	T3595	T3605	T3615	T3625	T3635	T3645	T3655	T3665	T3675	T3685	T3695	T3705	T3715	T3725	T3735	T3745	T3755	T3765	T3775	T3785	T3795	T3805	T3815	T3825	T3835	T3845	T3855	T3865	T3875	T3885	T3895	T3905	T3915	T3925	T3935	T3945	T3955	T3965	T3975	T3985	T3995	T4005	T4015	T4025	T4035	T4045	T4055	T4065	T4075	T4085	T4095	T4105	T4115	T4125	T4135	T4145	T4155	T4165	T4175	T4185	T4195	T4205	T4215	T4225	T4235	T4245	T4255	T4265	T4275	T4285	T4295	T4305	T4315	T4325	T4335	T4345	T4355	T4365	T4375	T4385	T4395	T4405	T4415	T4425	T4435	T4445	T4455	T4465	T4475	T4485	T4495	T4505	T4515	T4525	T4535	T4545	T4555	T4565	T4575	T4585	T4595	T4605	T4615	T4625	T4635	T4645	T4655	T4665	T4675	T4685	T4695	T4705	T4715	T4725	T4735	T4745	T4755	T4765	T4775	T4785	T4795	T4805	T4815	T4825	T4835	T4845	T4855	T4865	T4875	T4885	T4895	T4905	T4915	T4925	T4935	T4945	T4955	T4965	T4975	T4985	T4995	T5005	T5015	T5025	T5035	T5045	T5055	T5065	T5075	T5085	T5095	T5105	T5115	T5125	T5135	T5145	T5155	T5165	T5175	T5185	T5195	T5205	T5215	T5225	T5235	T5245	T5255	T5265	T5275	T5285	T5295	T5305	T5315	T5325	T5335	T5345	T5355	T5365	T5375	T5385	T5395	T5405	T5415	T5425	T5435	T5445	T5455	T5465	T5475	T5485	T5495	T5505	T5515	T5525	T5535	T5545	T5555	T5565	T5575	T5585	T5595	T5605	T5615	T5625	T5635	T5645	T5655	T5665	T5675	T5685	T5695	T5705	T5715	T5725	T5735	T5745	T5755	T5765	T5775	T5785	T5795	T5805	T5815	T5825	T5835	T5845	T5855	T5865	T5875	T5885	T5895	T5905	T5915	T5925	T5935	T5945	T5955	T5965	T5975	T5985	T5995	T6005	T6015	T6025	T6035	T6045	T6055	T6065	T6075	T6085	T6095	T6105	T6115	T6125	T6135	T6145	T6155	T6165	T6175	T6185	T6195	T6205	T6215	T6225	T6235	T6245	T6255	T6265	T6275	T6285	T6295	T6305	T6315	T6325	T6335	T6345	T6355	T6365	T6375	T6385	T6395	T6405	T6415	T6425	T6435	T6445	T6455	T6465	T6475	T6485	T6495	T6505	T6515	T6525	T6535	T6545	T6555	T6565	T6575	T6585	T6595	T6605	T6615	T6625	T6635	T6645	T6655	T6665	T6675	T6685	T6695	T6705	T6715	T6725	T6735	T6745	T6755	T6765	T6775	T6785	T6795	T6805	T6815	T6825	T6835	T6845	T6855	T6865	T6875	T6885	T6895	T6905	T6915	T6925	T6935	T6945	T6955	T6965	T6975	T6985	T6995	T7005	T7015	T7025	T7035	T7045	T7055	T7065	T7075	T7085	T7095	T7105	T7115	T7125	T7135	T7145	T7155	T7165	T7175	T7185	T7195	T7205	T7215	T7225	T7235	T7245	T7255	T7265	T7275	T7285	T7295	T7305	T7315	T7325	T7335	T7345	T7355	T7365	T7375	T7385	T7395	T7405	T7415	T7425	T7435	T7445	T7455	T7465	T7475	T7485	T7495	T7505	T7515	T7525	T7535	T7545	T7555	T7565	T7575	T7585	T7595	T7605	T7615	T7625	T7635	T7645	T7655	T7665	T7675	T7685	T7695	T7705	T7715	T7725	T7735	T7745	T7755	T7765	T7775	T7785	T7795	T7805	T7815	T7825	T7835	T7845	T7855	T7865	T7875	T7885	T7895	T7905	T7915	T7925	T7935	T7945	T7955	T7965	T7975	T7985	T7995	T8005	T8015	T8025	T8035	T8045	T8055	T8065	T8075	T8085	T8095	T8105	T8115	T8125	T8135	T8145	T8155	T8165	T8175	T8185	T8195	T8205	T8215	T8225	T8235	T8245	T8255	T8265	T8275	T8285	T8295	T8305	T8315	T8325	T8335	T8345	T8355	T8365	T8375	T8385	T8395	T8405	T8415	T8425	T8435	T8445	T8455	T8465	T8475	T8485	T8495	T8505	T8515	T8525	T8535	T8545	T8555	T8565	T8575	T8585	T8595	T8605

Since LWC meter readings are considered indeterminate above -5°C, near freezing temperature data were obtained by running equivalent water-flow rates.

The following is a typical flight profile:

1. Aircraft is fueled up to max gross weight.
2. After engine startup, bleed air is feed into air and water supply lines to prevent system freeze-ups.
3. The estimated water-flow rate required for the first part of the test is set during climb-out.
4. Aircraft climbs to the desired OAT level and then levels out at the test airspeed.
5. Bleed air pressure is then set to estimated value and water is directed into spray rig.
6. Bleed air to water line is disconnected.
7. Water-flow rate is now adjusted if required to desired liquid water meter reading.
8. Using oil slides, ice cloud droplet samples are taken, checked for size and photographed using a shock mounted microscope. If necessary, bleed air pressure is adjusted and above procedure is repeated.
9. All required aircraft and spray rig data are manually recorded. Videos of the inlet screen are taken through the aft cabin window.
10. Steps 8 through 10 are repeated for the second part of the conditions.
11. After all required data are taken, the water supply line and water passages in the spray rig are purged with bleed air.
12. After landing, the ice buildup on various inductions system parts is observed and photographically documented.

6.4 DROPLET QUALITY.

Oil slide pictures taken during FAA testing have been placed on file at Heli-Air. Even though the time lapse between obtaining the droplet sample and taking the picture was only about 5 seconds, some droplet size distortion due to coalescence and evaporation could be observed. While the latter increases MVD somewhat, the former may result in very large drops which will not only significantly increase MVD, but will also result in a rather lopsided and erratic droplet size distribution. For this reason, it was decided to ignore the two largest droplets on each slide as far as MVD tabulations and calculations were concerned.

Figure 16 shows the droplet sizes measured for each test condition versus liquid water content. By and large, this figure shows that droplet size targets have been met, and that nozzle performance could be controlled within the tested liquid water contents.

Figure 17 shows that the droplet size distributions of the "small" droplet runs compare fairly well to that found in a "standard" stratiform cloud.

6.5 TEMPERATURE.

The ice cloud air temperature was measured by an aft facing thermocouple mounted on the 8-inch-long rod (item 4, figure 12) and a thermocouple on the inner screen of the engine inlet. As expected, the former temperature reads slightly higher, and the latter temperature somewhat lower than OAT. This effect is assumed to be mainly due to evaporation.

From ice shapes observed and calculations, one may conclude that water droplet impact temperatures were sufficiently close to ambient temperatures, and that these ice tests did simulate natural icing conditions fairly well.

6.6 INLET PERFORMANCE.

6.6.1 Photographic and Visual Records.

The ice buildup on the inlet screen was observed and photographed using a video camera via a wing mounted mirror. The videos are on file at Heli-Air.

After each condition, the aircraft landed and the photographs shown in figures 18 through 24 were taken.

A summary of observations based on visual and photographic evidence is presented in table 4. The tabulated open areas are estimated from the photographs.

6.6.2 Inlet Losses.

Table 5 shows the temperature rise caused by ice buildup on the air induction system. Inlet losses were deduced from various observations. Estimates under "average" values demonstrate sufficient temperature margins to fly the aircraft even under the most severe icing conditions for the time interval anticipated.

7. CONCLUSION/OBSERVATIONS.

The inlet loss data obtained during these tests were rather sketchy and only moderately verifiable. Nevertheless, the effects of various parameters on the inlet configuration tested could be evaluated.

The overall effect of an increase in airspeed showed a small decrease in inlet losses. This is, as expected, particularly true for the larger droplet sizes. The difference in blockage due to ice buildup on the inlet slot and inner

RUN	OUTER SCREEN	% OPEN	BYPASS CAP	% OPEN	INNER SCREEN	% OPEN
5A	Pressure loss in excess of 27' - Granular rime ice.	0	Distinct secondary stagnation stream line-	75	4" elliptical area with ~15' ice build-up upon wire - very little bridging.	95
5B	Heavier ice build-up than previous run. Coarser rime ice which appeared to be self-clearing. Pressure loss in excess of 27'. Max loss appears to be somewhat less than for run 5A.	6	Less pronounced stagnation stream line. More ice build-up on aft section of gap.	95	About the same as Run 5A. Some bridging.	85
5C	Intermediate amount of ice build-up of rather finely structured rime ice. Screen was self cleaning around the periphery.	9	Ice shape similar to Run 5B.	95	Wire ice build-up extensive over a larger area, but there was no bridging.	93
5D	Larger amount of very coarse and porous, almost translucent rime ice.	10	Only a small amount of ice on gap surface.	100	No ice on inner screen.	100
5E	About the same amount of ice build-up as run 5D, but with a much finer, still porous rime ice structure.	2	Fair amount of ice on gap surface rather uniformly distributed.	90	Considerable ice build-up on inner screen, but relatively little bridging.	70
6A	Screen sheds ice during test. Relatively low ice accumulation with large open areas.	20	Almost completely ice free.	100	Slight frost on wires.	98
6B	Higher ice accumulation - Less shedding.	8	Some ice accumulation.	100	Very little frost on screen wires.	99
6D	No photograph.	-	-	-	-	-

Table 4. Bell 222/Allison 250-C30G Ice Build-Up Test Results Summary - Sheet 1 of 2

RUN	OUTER SCREEN	% OPEN	BYPASS GAP	% OPEN	INNER SCREEN	% OPEN
7A	Very fluffy rime ice which circumcised easily on contact. Shedding during run.	0	Pronounced stagnation line build-up on forward part of gap area.	85	Considerable ice build-up over approximately 80% of screen area but without bridging.	65
7B	Same as 7A.	0	Two ice ridges in gap. Appears to be worse than Run 7A.	80	Significant amount of screen is iced over.	65
8A	Screen completely covered with rime ice.	0	Only small ridge of ice on forward part of gap.	98	Center part iced over, clean around perimeter.	55
9A	Gloze ice over entire screen.	0	Essentially ice free except for small area on top.	100	About 20% clear, 50% iced up, but no bridging and about 30% broken off.	50
9B	Same as 9A.	0	Clear gap.	100	Slightly iced up.	98

Table 4. Bell 222/Allison 250-C30G Ice Build-Up Test Results Summary - Sheet 2 of 2

COND	TOT RISE - °C			
	A	B	C	AVERAGE
5A	40	41	20	34
5B	43	34	30	36
5C	15	19	-	17
5D	25	21	20	22
5E	18	29	40	29
6A	10	7	5	7
6B	30	8	5	14
7A	29	29	15	24
7B	33	34	20	29
8A	12	19	-	16
9A	12	19	-	16
9B	11	21	-	16

NOTE:

- A - The total pressure loss as measured by a single duct-mounted pitot tube and the engine performance deck are the basis for these values.
- B - This TOT rise is based on estimated open areas and the engine deck.
- C - Measured temperature rise.
(Pilots TOT gage.)

Table 5. Bell 222/Allison 250-C30G Inlet Losses due to Icing

screen apparently more than offset the inherently higher losses associated with the aft facing slot. It is therefore concluded that the aircraft should, if inadvertent ice penetration occurs, fly at about 60 to 70 KIAS. Since this range is near maximum endurance speed for most conditions, lower power requirements will also tend to increase the already large TOT margins.

The results obtained clearly show the much higher inertial separation efficiencies for the larger droplet sizes if compared at constant airspeeds.

Conditions flown at just below freezing temperatures are generally assumed to be critical for screened inlets. This appears to be the case, especially with large droplet sizes. Current test results show, however, that this is not necessarily true. The very fine mesh outer screen was very quickly closed off by a layer of glaze ice. Any runback was then apparently shed externally.

The effect of slot configuration was evaluated by testing two different screen sizes. The larger screen was designed to minimize slot losses under icing conditions and maximize droplet separation efficiency. It was clearly the better screen.

Since, on a two-engine helicopter, power demands per engine are relatively low, the 34°F maximum TOT temperature rise allows sufficient margin to assure adequate engine performance throughout the flight envelope.

To check if remelting of ice accumulations acquired during an inadvertent icing encounter would affect engine performance, a test point equivalent to run 5A was flown. After landing, the iced up engine was kept running at 40 percent torque levels while the inlet was deiced using a portable heater. No adverse engine reactions were observed.

8. REFERENCES.

1. Federal Aviation Administration "Certification of Transport Category Rotorcraft," Advisory Circular AC-29-2A paragraph 532.
2. Federal Aviation Regulations Part 29 paragraph 1093 (b)(1)(i)
3. Federal Aviation Regulation Part 25, Appendix C
4. Leigh Instrument LTD "Operational Manual, MK12B Ice Detector System IDU-3B," Careton Place, Ontario, Canada.
5. "Spray Nozzle and Accessories," Industrial Catalog 27, Spraying Systems CO., North Avenue at Scmale Road, Wheaton, IL.

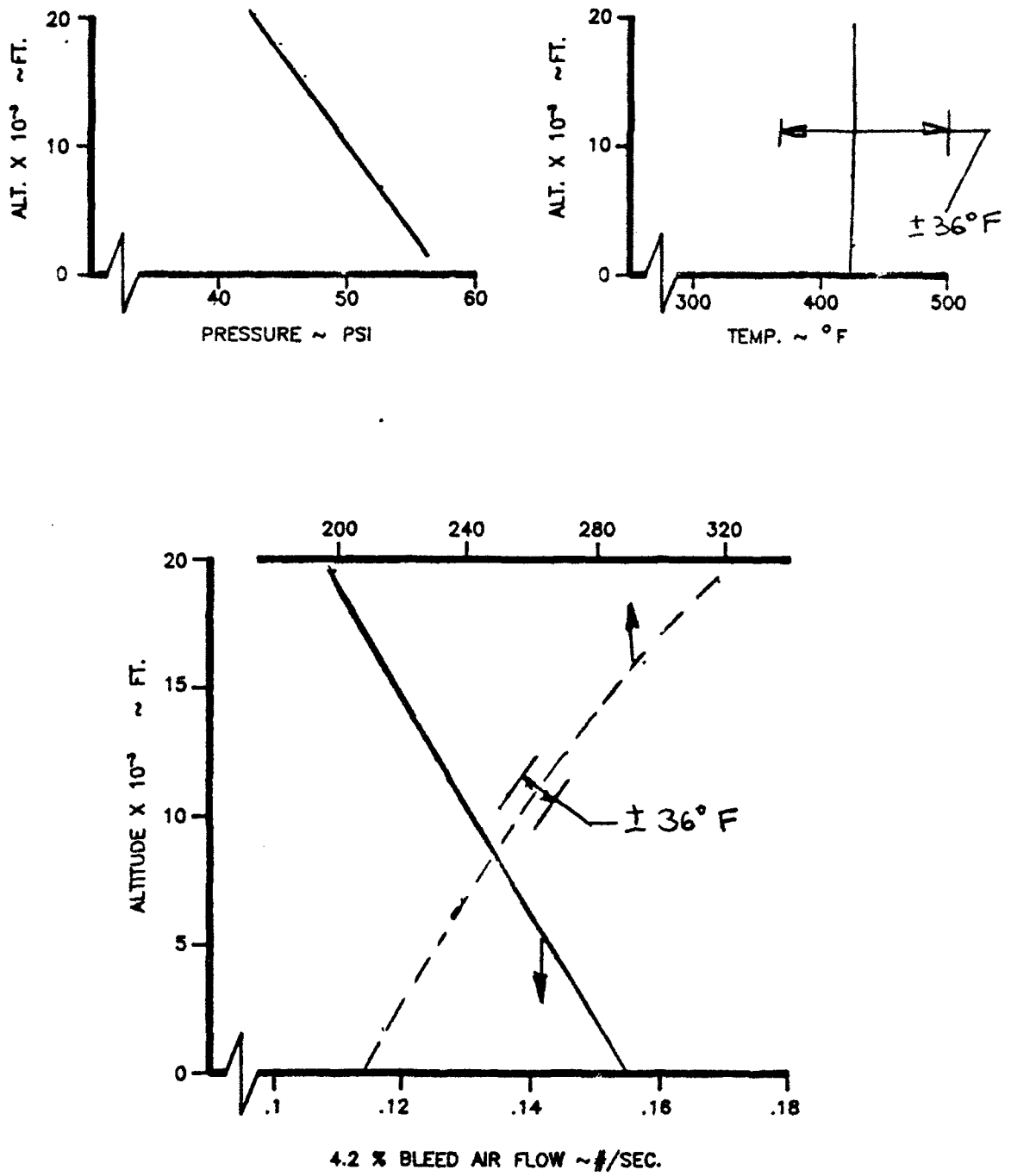


Figure 1. Available Bleed Air per Engine
at 60 KIAS - 4.2% Bleed, Std. Day.

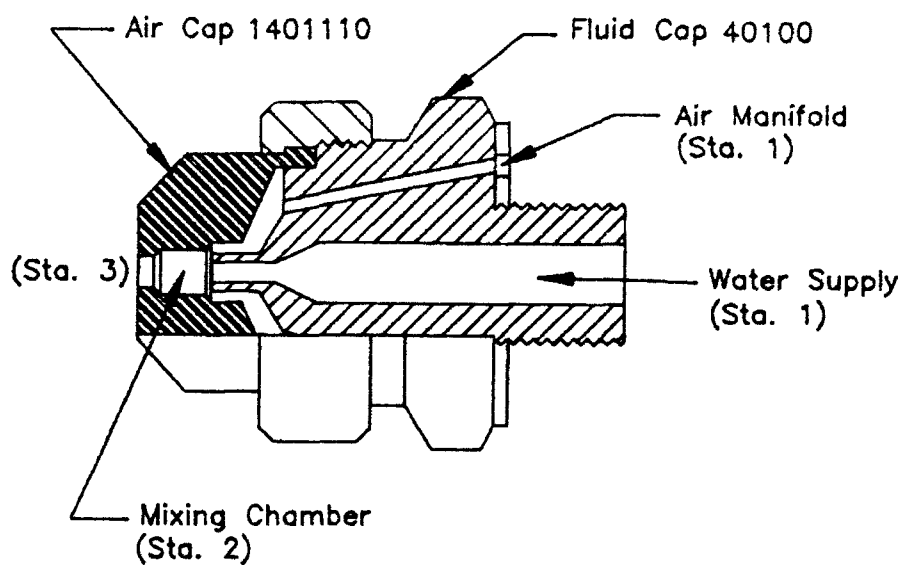


Figure 2. Spray Nozzle

REF.: SPRAYING SYSTEMS Co.
SETUP 22B

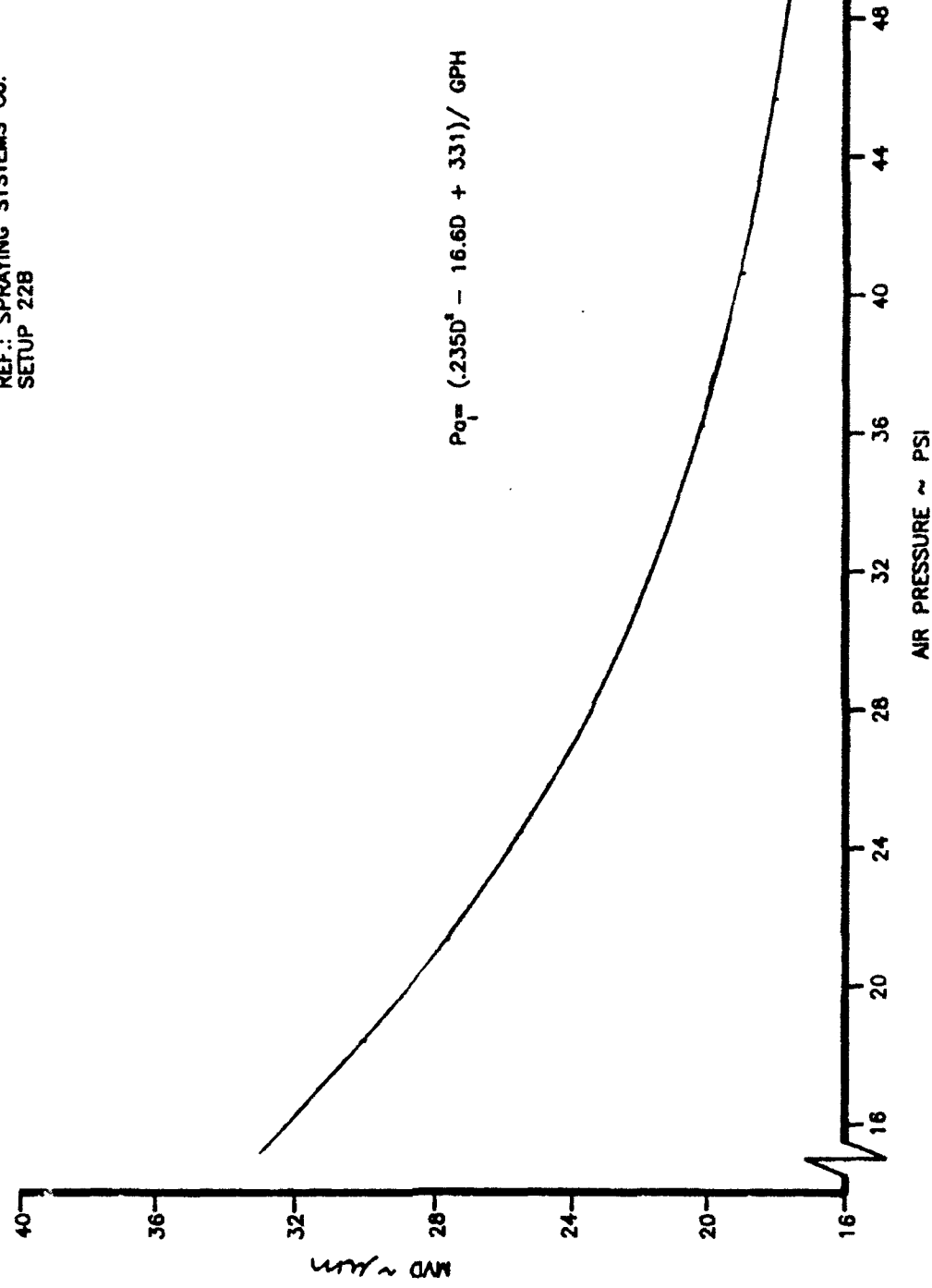


Figure 3. Spray Nozzle Performance (GPH = 2.5)

```

5 CLS
10 REM           ICE TEST RIG EVALUATION
20 REM
30 REM X=INDEX ON AIR SUPPLY PRESSURE      (PA1)      (MAX=N)
40 REM Y=INDEX ON NUMBER OF STEPS (JET PATH)          (MAX=M)
50 REM
60 REM ***** INITIAL CONDITIONS *****
70 REM
80 INPUT"WATER FLOW RATE PER NOZZLE          [GPH]      =":GPH
90 INPUT"INITIAL WATER TEMPERATURE          (RAKE)     [DEG F]      =":1TO
100 INPUT"INITIAL BLEED AIR TEMPERATURE      (RAKE)     [DEG F]      =":1TA1
110 INPUT"AIRSPEED                          [KIAMS]     =":1VO
130 INPUT"DISTANCE TO TARGET                [INCHES]    =":1XF
140 INPUT"WATER DROPLET SIZE                [MICRONS]   =":1D
150 INPUT"PRESSURE ALTITUDE                [FT]        =":1HP
155 INPUT"DAT                               [DEG F]      =":1DAT
160 N=1
170 M=100
175 DIM E(M+2,11)
180 RC=.9
190 DPA1=10
200 RX=53.3
210 CP=.24
220 P0=30
230 ROH=62.4
240 VIS=3.5E-07
250 PR=.71
260 K=1.4
270 KH=.0273
280 G=32.2
285 K1=18*3.5E-07/(ROH*3.2808E-06^2)
286 E1=2.7183
290 REM
300 REM ***** NOZZLE DIMENSIONS *****
310 REM *
311 REM * THE NOZZLE USED FOR THIS PROGRAM WAS OF THE INTERNAL MIX TYPE *
312 REM * AND WAS MANUFACTURED BY THE SPRAYING SYSTEMS COMPANY *
313 REM *           SETUP 22B *
314 REM *****
320 D1=.04
330 D2=.1
340 D3=.14
350 D4=.11
360 A1=(.7854*D1^2)/144
370 A2=(.7854*(D3^2-D2^2))/144
380 A3=(.7854*D4^2)/144
390 REM
400 REM ***** CALCULATIONS OF NOZZLE EXIT CONDITIONS *****
410 REM
420 THET=1-1.416*8.875E-06
430 DELT=THET^5.2561
440 SIGMA=THET^4.2561
450 VR=V0*1.688/SOR(SIGMA)
460 F2=2116*DELT
470 A=2*G*K/(K-1)

```

Figure 4. Code to calculate droplet impact conditions, Sheet 1 of 3.

```

480 C1=2/K
490 C2=(K-1)/K
500 T=TA1+460
505 TA=DAT+460
510 PA1=P0
520 WW=8.345*GPH/3600
530 VW2=WW/(ROH*A1)
531      LPRINT"           ICE RIG EVALUATION - PATH"
532      LPRINT
535      LPRINT"X","V[DRPLT]","T[DRPLT]","VA[DELTA]"
536      LPRINT"[INCHES]","[KIAS]","[DEG F]","[KIAS]"
540 FOR X=1 TO N
550   PA1=PA1+DFA1
560   PW1=.572*PA1+2.56*GPH-7.4
570   PW=PW1*144+P2
580   PC=FW-(WW/A1)^2)/(2*G*ROH)
590   P1=PA1*144+P2
600   R=PC/P1
610   TA2=T*(1-RC*(1-R^C2))
620   WA=.7*P1*A2*SQR((A*R^C1/(RX*T))*(1-R^C2))
630   CFM=WA*RX*TA2*60/P2
640   VA2=SQR(A*RX*T*(1-R^C2))
650   M2=VA2/(49.1*SQR(T))
660   REM
670   REM LET TA2=TA3 (CONSERVATIVE FOR IMPACT TEMPERATURES)
680   REM
690   VA3=WA*TA2*RX/(PC*(A3-A1))
695 GOSUB 3000
700 E(X,5)=PA1
705 E(X,6)=PW1
710 E(X,7)=VA3
720 E(X,8)=VWI
730 E(X,9)=TWI
735 E(X,10)=CFM
740 NEXT X
800 OPEN "LPT1;" AS #1
805 PRINT#1,
810 REM PRINT#1,"           ICE TEST RIG EVALUATION"
820 PRINT#1,
830 PRINT#1,"WATER FLOW RATE PER NOZZLE      [GPH]    =";GPH
840 PRINT#1,"INITIAL WATER TEMPERATURE AT RAKE   [DEG F]  =";TO
850 PRINT#1,"INITIAL BLEED AIR TEMPERATURE AT RAKE [DEG F]  =";TA1
860 PRINT#1,"AIRSPEED          [KIAS]   =";VO
880 PRINT#1,"DISTANCE TO TARGET        [INCHES] =";XF
890 PRINT#1,"PRESSURE ALTITUDE        [FT]     =";HP
900 PRINT#1,"DAT             [DEG F]   =";DAT
910 PRINT#1,"WATER DROPLET SIZE       [MICRONS] =";D
920 PRINT#1,
930 PRINT#1,"PA1","PW1","VA[EXIT]", "CFM"
940 FOR S=1 TO N
950   PRINT#1,E(S,5),E(S,6),E(S,7),E(S,10)
960 NEXT S
970 PRINT#1,
980 PRINT#1,"PA1","V[IMPACT]","T[IMPACT]"
990 FOR S=1 TO N

```

Figure 4. Code to calculate droplet impact conditions, Sheet 2 of 3.

```

1000 PRINT#1,E(S,5),(E(S,8)*SDR(SIGMA)/1.688),(E(S,9)-460)
1010 NEXT S
1020 END
3000 REM
3010 REM ***** ROUND JET TRAJECTORY *****
3020 REM
3030 B1=.174533*B
3040 V=VA3
3060 DX=XF/M
3070 FOR S=1 TO M
3080 U=1
3120 S1=S1+DX
3130 KJ=1
3150 KJ=6*D4/S1
3160 IF KJ>1 THEN KJ=1
3170 IF KJ>1 THEN KJ1=1 ELSE KJ1=5*KJ/6
3180 TJ=KJ1*(TA2-TA)+TA :REM JET CORE TEMPERATURE
3190 VAJ=KJ*(VA3-VR)+VR :REM JET CORE VELOCITY (MAX)
3240 E(S,0)=S1
3250 E(S,1)=VAJ
3255 E(S,2)=TJ
3270 NEXT S
3271 V=VA3
3272 S1=0
3273 TJ=TA2
3280 REM
3290 REM ***** WATER DROPLET VEL.& TEMP *****
3300 REM
3310 REM
3320 E(0,1)=VA3-VR :REM NOZZLE EXIT VELOCITY OF AIR
3330 E(0,2)=TA2 :REM NOZZLE EXIT TEMPERATURE OF AIR
3340 E(0,3)=VW2 :REM NOZZLE EXIT VELOCITY OF WATER
3350 E(0,4)=T0+460 :REM NOZZLE EXIT TEMPERATURE OF WATER
3360 FOR S=1 TO M
3370 BJ=K1*E(S,0)/D^2
3380 CJ=E(S-1,3)^2+BJ*(E(S,1)+E(S-1,1)-E(S-1,3)) :REM VW=DROPLET VELOCITY AT S
3390 E(S,3)=.5*(-BJ+SDR(BJ^2+4*CJ)) :REM AVERAGE DIFFERENCE IN VEL
3400 VARW=(E(S,1)+E(S-1,1)-E(S,3)-E(S-1,3))/2 :REM AVERAGE JET CORE TEMP.
3410 TAJ=(E(S-1,2)+E(S,2))/2 :REM AVERAGE REYNOLDS NUMBER
3420 RN=(P2/TAJ)*ABS(VARW)*D/183.1 :REM AVERAGE PRANDL NUMBER
3430 NU=2+.4*RN^(1/2)+.06*RN^(2/3)*PR^.4 :REM AVERAGE FILM COEFFICIENT
3440 HC=4!*NU/D :REM AVERAGE JET CORE VELOCITY
3450 VWA=(E(S,3)+E(S-1,3))/2 :REM TIME REQUIRED TO TRAV. DX
3460 TT=DX/VWA
3470 L=29322*HC*TT/D
3475 IF L>80 THEN L=80
3480 E(S,4)=(E(S-1,4)-TAJ)*E1^(-L)+TAJ :REM IMPACT TEMPERATURE
3481 PRINT E1,E1^(-L),E(S-1,4)-TAJ,HC
3482 TWI=E(S,3)
3488 TWI=E(S,4)
3489 LPRINT E(S,0),(VW1*SDR(SIGMA)/1.688),(TWI-460),(VARW*SDR(SIGMA)/1.688)
3490 NEXT S
3500 RETURN

```

Figure 4. Code to calculate droplet impact conditions, Sheet 3 of 3.

ICE FIG EVALUATION - PATH

X [INCHES]	[INAS]	TCDPLT]	LDEG F1	LDEG A8J	VALDELTAJ	VALDELTAI	16.875E-01	16.453E-01
.84	59.84319	144.86601	263.89668				46.20001	46.20001
1.68	88.08549	92.9057	155.329				47.00001	47.00001
2.52	110.00357	59.54901	55.5628				48.72001	48.72001
3.36	104.5867	47.17063	17.43				54.13154	54.13154
4.2	104.3653	40.92877	-6.6879428				49.36001	49.36001
5.04	100.9033	35.95783	-6.806998				54.06115	54.06115
5.88	95.52702	32.89324	-11.21811				50.40001	50.40001
6.72	89.43594	30.66956	-10.46642				51.24001	51.24001
7.56	83.62683	29.02826	-8.31089				52.08001	52.08001
8.40	78.71036	27.74457	-5.934724				53.8022	53.8022
9.24	74.98055	26.71121	-3.9763048				53.76001	53.76001
10.08	72.00604	25.86029	-2.616312				53.37228	53.37228
10.92	69.83205	25.14559	-1.7637865				53.42533	53.42533
11.76	68.12875	24.53912	-1.248089				61.322001	61.322001
12.6	66.74041	24.01575	-9.282106				62.16001	62.16001
13.44	65.51526	23.54624	-7.716945				53.25819	53.25819
14.28	64.5707	23.16025	-5.7050569				63.00001	63.00001
15.12	63.6977	22.80425	-4.6227848				63.84001	63.84001
15.96	62.92607	22.49021	-3.814021				64.48601	64.48601
16.8	62.24375	22.20773	-3.164703				65.52001	65.52001
17.64	61.63067	21.95235	-2.689126				66.36	66.36
18.48	61.02786	21.72119	-2.292804				52.99188	52.99188
19.32	60.57656	21.5105	-1.9171725				68.04	68.04
20.16	60.11569	21.31784	-1.708473				68.67999	68.67999
21.	59.70147	21.14093	-1.490514				69.71999	69.71999
21.84	59.31706	20.978	-1.308447				70.55998	70.55998
22.68	58.96247	20.82239	-1.155029				71.39998	71.39998
23.52	58.63429	20.66778	-1.024929				72.23998	72.23998
24.36	58.32961	20.53798	-9.137926E-02				73.07997	73.07997
25.2	58.04598	20.43707	-8.181608E-02				52.88351	52.88351
26.04	57.78124	20.32407	-7.354698E-02				52.68869	52.68869
26.88	57.53359	20.21826	-6.637255E-02				75.59996	75.59996
27.72	57.30133	20.11902	-6.009341E-02				76.43996	76.43996
28.56	57.08313	20.0257	-5.458339E-02				52.78268	52.78268
29.4	56.87765	19.93781	-4.974076E-02				78.19995	78.19995
30.24	56.6839	19.85486	-4.054475				52.51542	52.51542
31.08	56.50098	19.77649	-3.016385				79.79995	79.79995
31.92001	56.32764	19.7023	-3.024866E-02				80.63994	80.63994
32.76	56.16348	19.63196	-3.520879E-02				52.49229	52.49229
33.6	56.00765	19.56519	-3.0324904				82.31993	82.31993
34.44	55.85955	19.50174	-3.060046				83.15993	83.15993
35.28	55.71863	19.44138	-2.783099E-02				83.99992	83.99992
36.12	55.58438	19.38382	-2.584094E-02				52.39244	52.39244
36.96	55.4563	19.32895	-2.403411E-02				52.64034	52.64034
37.8	55.33599	19.27655	-2.238599E-02				52.57285	52.57285
38.64	55.21709	19.22641	-2.0886943E-02				78.09442	78.09442
39.48	55.10521	19.17847	-1.955517E-02				52.6827	52.6827
40.32	54.99805	19.13254	-1.6277992E-02				52.51856	52.51856
41.16	54.8953	19.0885	-1.715234E-02				18.07123	18.07123
42.00001	54.79673	19.04623	-1.607429E-02				52.44133	52.44133
42.84001	54.70264	19.00568	-1.015139				52.41666	52.41666
43.68001	54.61106	19.96671	-1.422676E-02				18.02771	18.02771
PAL	PW1	VAL EXIT J	CFM				664.1588	6.532487
FAL	40	21.88						

Figure 5. Droplet Trajectory Calculations,
MVD = 25

CE RIG EVALUATION - PATH		VALDELTAB [K1AB]	
X [INCHES]	Y [INCHES]	TDRPLT1 CK1AB, C DEG F1	VALDELTAB [K1AB]
54.46157	-4.18238E-02	54.46157	54.46157
54.38465	-3.946135E-02	54.38465	54.38465
54.30511	-3.72403E-02	54.30511	54.30511
54.22827	-3.524949E-02	54.22827	54.22827
54.15415	-3.333369E-02	54.15415	54.15415
54.08261	-3.162158E-02	54.08261	54.08261
54.0135	-2.995584E-02	54.0135	54.0135
53.9597	-2.847183E-02	53.9597	53.9597
53.94671	-2.6421262	53.94671	53.94671
53.88214	-2.0270577	53.88214	53.88214
53.81966	-1.0257331	53.81966	53.81966
53.75918	-2.449394E-02	53.75918	53.75918
53.70058	-2.0233362	53.70058	53.70058
53.64381	-2.224559E-02	53.64381	53.64381
53.58975	-25.42612	53.58975	53.58975
53.53536	-2.026581E-02	53.53536	53.53536
53.48354	-1.936646E-02	53.48354	53.48354
53.43321	-1.852002E-02	53.43321	53.43321
53.38435	-1.771427E-02	53.38435	53.38435
53.33685	-1.696142E-02	53.33685	53.33685
53.29067	-1.625334E-02	53.29067	53.29067
53.24575	-1.557374E-02	53.24575	53.24575
53.20266	-1.493484E-02	53.20266	53.20266
53.15954	-1.433664E-02	53.15954	53.15954
53.11914	-1.377098E-02	53.11914	53.11914
53.0778	-1.322568E-02	53.0778	53.0778
53.03852	-1.271295E-02	53.03852	53.03852
53.00022	-1.223274E-02	53.00022	53.00022
52.96287	-1.176475E-02	52.96287	52.96287
52.92646	-1.133339E-02	52.92646	52.92646
52.89092	-1.091631E-02	52.89092	52.89092
52.85624	-1.051346E-02	52.85624	52.85624
52.82241	-1.013697E-02	52.82241	52.82241
52.78934	-9.776863E-03	52.78934	52.78934
52.75705	-9.428891E-03	52.75705	52.75705
52.72552	-9.103336E-03	52.72552	52.72552
52.69095	-8.798128E-03	52.69095	52.69095
52.65649	-8.496989E-03	52.65649	52.65649
52.62454	-8.196989E-03	52.62454	52.62454
52.63567	-8.216198E-03	52.63567	52.63567
52.60626	-7.943546E-03	52.60626	52.60626
52.57807	-7.687171E-03	52.57807	52.57807
52.55049	-7.438935E-03	52.55049	52.55049
52.52346	-7.198838E-03	52.52346	52.52346
52.49703	-6.962811E-03	52.49703	52.49703
52.47994	-6.743061E-03	52.47994	52.47994
52.44558	-6.539589E-03	52.44558	52.44558
52.42096	-6.336117E-03	52.42096	52.42096
52.39663	-6.140784E-03	52.39663	52.39663
PW1	VAL1X11		
40	21.88	064.1568	6.532487
PA1	V1IMFACT1	52.39663	2B.95014

Figure 6. Droplet Trajectory Calculations,
MVD = 45

```

10 REM
20 REM "      ESTIMATED ICE RIG SETTINGS"
30 REM
40 CLS
50 INPUT"GRAMS OF WATER PER M^3"           [GRAM]   ="1GR
60 INPUT"ICING CLOUD SIZE"                 [FT 2]   ="1AC
70 INPUT"AIRSPEED"                         [KIAS]   ="1V
80 INPUT"DAT"                             [DEG F]   ="1DAT
90 INPUT"OAT"                            [FT]     ="1HP
100 INPUT"ALTITUDE"                      [MICRONS] =;"1D
110 INPUT"DESIRED DROPLET DIAMETER"       [DEG F]   ="1TA1
115 INPUT"BLEED AIR TEMPERATURE"          120 RG=53.3
130 K=1.4
140 G=32.2
141 D1=.04
143 D2=.1
145 D3=.14
147 D4=.11
150 THET=1-HF*6.875E-06
160 DELT=THET*.2561
170 SIGMA=DELT*518/(460+OAT)
200 GPHT=.0455*GR*V*AC/SOR(SIGMA)
201 N=GPHT/2.5
205 GPH=2.5
210 PA1=(9.39999E-02*D^2-6.64*D+132.2)*GPH/2.5
220 PW1=.572*PA1+2.56*GPH-7.4
230 WA=.0766*SOR(SIGMA)*V*1.688*AC
240 P2=2116*DELT
250 A1=(-.7854*D1^2)/144
260 A2=(-.7854*D2^2)/144
270 A3=(-.7854*D3^2)/144
280 A4=(-.7854*D4^2)/144
290 P2=2116*DELT
300 A=2*G*K/(K-1)
310 C1=2/K
320 C2=(K-1)/K
330 T=460+TA1
340 WM=0.345*2.5/3600
350 FW=PW1*144+P2
355 PI=PA1*144+P2
360 PC=PW-((WM/A1)^2)/(G*62.382)
370 R=PC/PI
380 TA2=T*(1-.98*(1-R*C2))
390 WA1=.78*1*A2*SOR((A*R*C1/(RG*T)))*(1-R*C2))
400 CFM=WA1*RG*TA2*60*IN/P2
2350 LPRINT
2400 LPRINT
2450 LPRINT" ##### TEST PARAMETERS #####
2500 LPRINT
2550 LPRINT"GRAMS OF WATER PER M^2"           [GRAM]   ="1GR
2600 LPRINT"ESTIMATED ICING CLOUD SIZE"       [FT 2]   ="1AC
2650 LPRINT"AIRSPEED"                         [KIAS]   ="1V
2700 LPRINT"DAT"                             [DEG F]   ="1DAT
2750 LPRINT"DROPLET SIZE"                    [MICRONS] =;"1D
2755 LPRINT"BLEED AIR RAKE TEMPERATURE"       [DEG F]   ="1TA1
2800 LPRINT
2850 LPRINT
2900 LPRINT" ##### ICE RIG CONFIGURATION #####
2950 LPRINT
3000 LPRINT"OPTIMUM NUMBER OF NOZZLES"         [IN]     ="1N
3100 LPRINT"BLEED AIR PRESSURE AT NOZZLE"      [PSI]    ="1PA1
3200 LPRINT"WATER SUPPLY PRESSURE AT NOZZLE"    [PSI]    ="1PWI
3210 LPRINT"WATER FLOW RATE"                   [X]      ="1(1.38*GPH)
3300 LPRINT"FLOW RATE OF ICING CLOUD AT INLET"  [/SEC]   ="1WA
3350 LPRINT"BLEED AIR FLOW REQUIRED"            [CFM]    ="1CFM
3400 END

```

Figure 7. Design Code for Ice Rig

***** TEST PARAMETERS *****

GRAMS OF WATER PER M ⁻²	[GRAM]	= 2.5
ESTIMATED ICING CLOUD SIZE	[FT ²]	= 9
AIRSPEED	[KIAS]	= 100
QAT	[DEG F]	= 17
DROPLET SIZE	[MICRONS]	= 20
BLEED AIR RHE TEMPERATURE	[DEG F]	= 250

***** ICE RIG CONFIGURATION *****

OPTIMUM NUMBER OF NOZZLES	[PSI]	= 29.82241
BLEED AIR PRESSURE AT NOZZLE	[PSI]	= 38.99994
WATER SUPPLY PRESSURE AT NOZZLE	[PSI]	= 29.16374
WATER FLOW RATE	[G]	= 102.889
FLOW RATE OF ICING CLOUD AT INLET	[#/SEC]	= 71.01745
BLEED AIR FLOW REQUIRED	[CFM]	= 191.0099

Figure 8. Typical Output from Design Code (Figure 7).

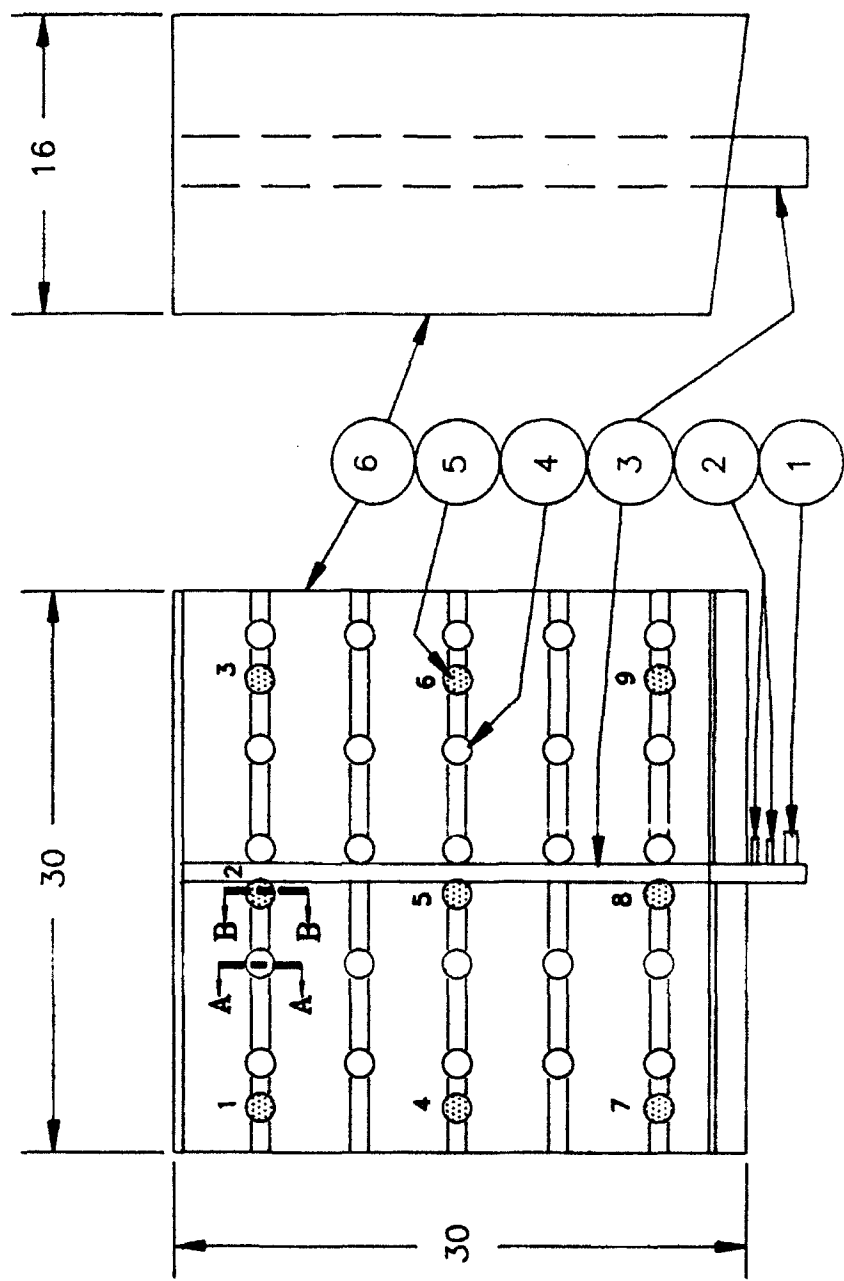
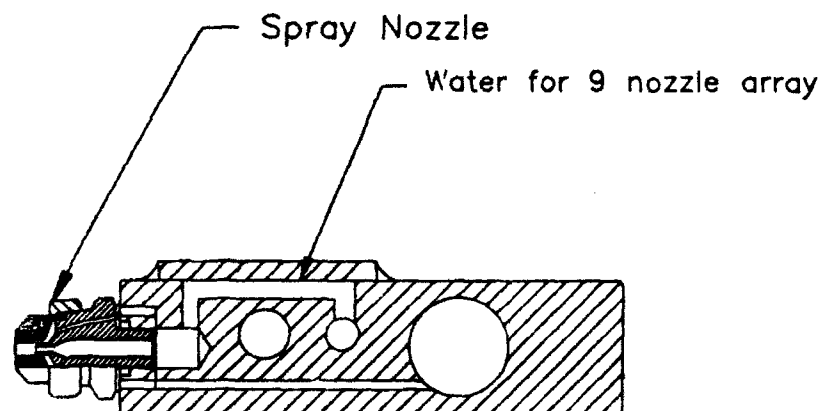
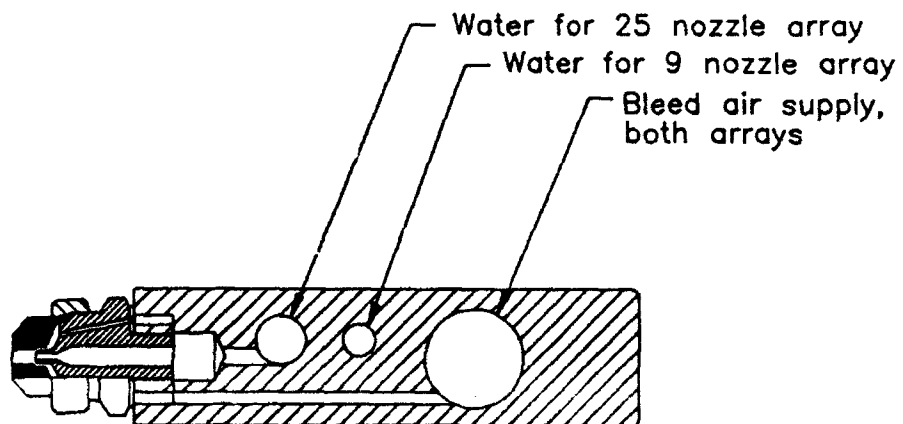


Figure 9. Spray Rake Configuration

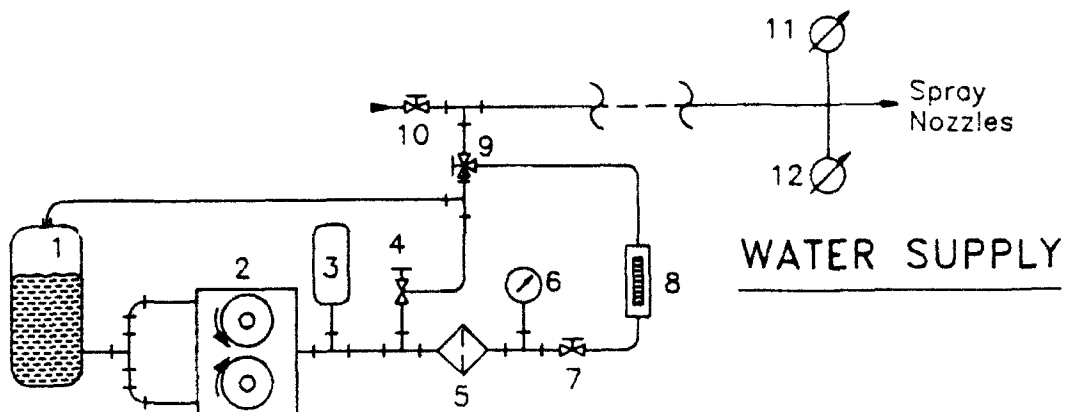


SECTION A-A

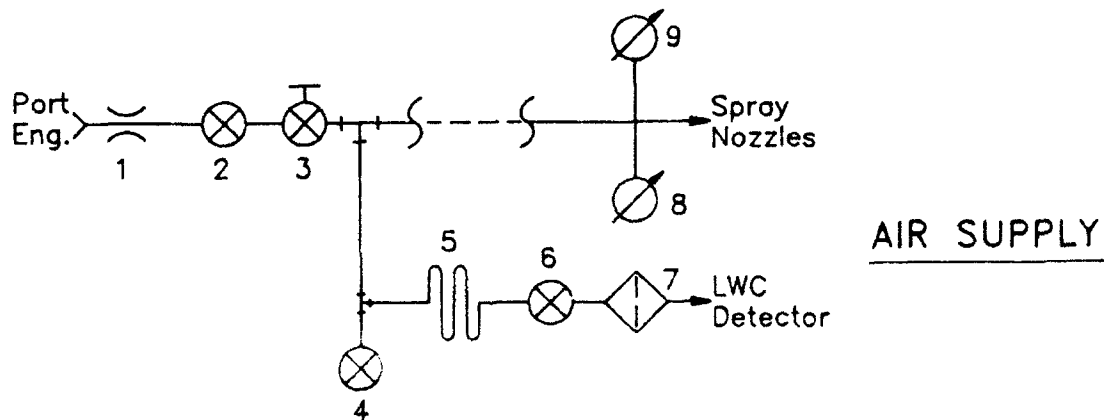


SECTION B-B

Figure 10. Nozzle Feed Details



1. 30 gallon ventilated water tank
2. Double-acting, variable, positive displacement water pump
3. Accumulator
4. Pressure relief valve
5. Water filter
6. Pressure gauge
7. Metering valve
8. Flow meter
9. Three-way valve
10. Bleed-air shut-off valve
11. Thermocouple
12. Pressure pick-up



1. Bleed air orifice ($d = 0.435$ in.)
2. Bleed air shut-off
3. Bleed air control valve
4. Water trap
5. Cooling coils
6. Shut off valve
7. Filter for LWC meter (see inst. man.)
8. Thermocouple
9. Pressure pick-up

Figure 11. Test Equipment Schematic

* Patent Pending

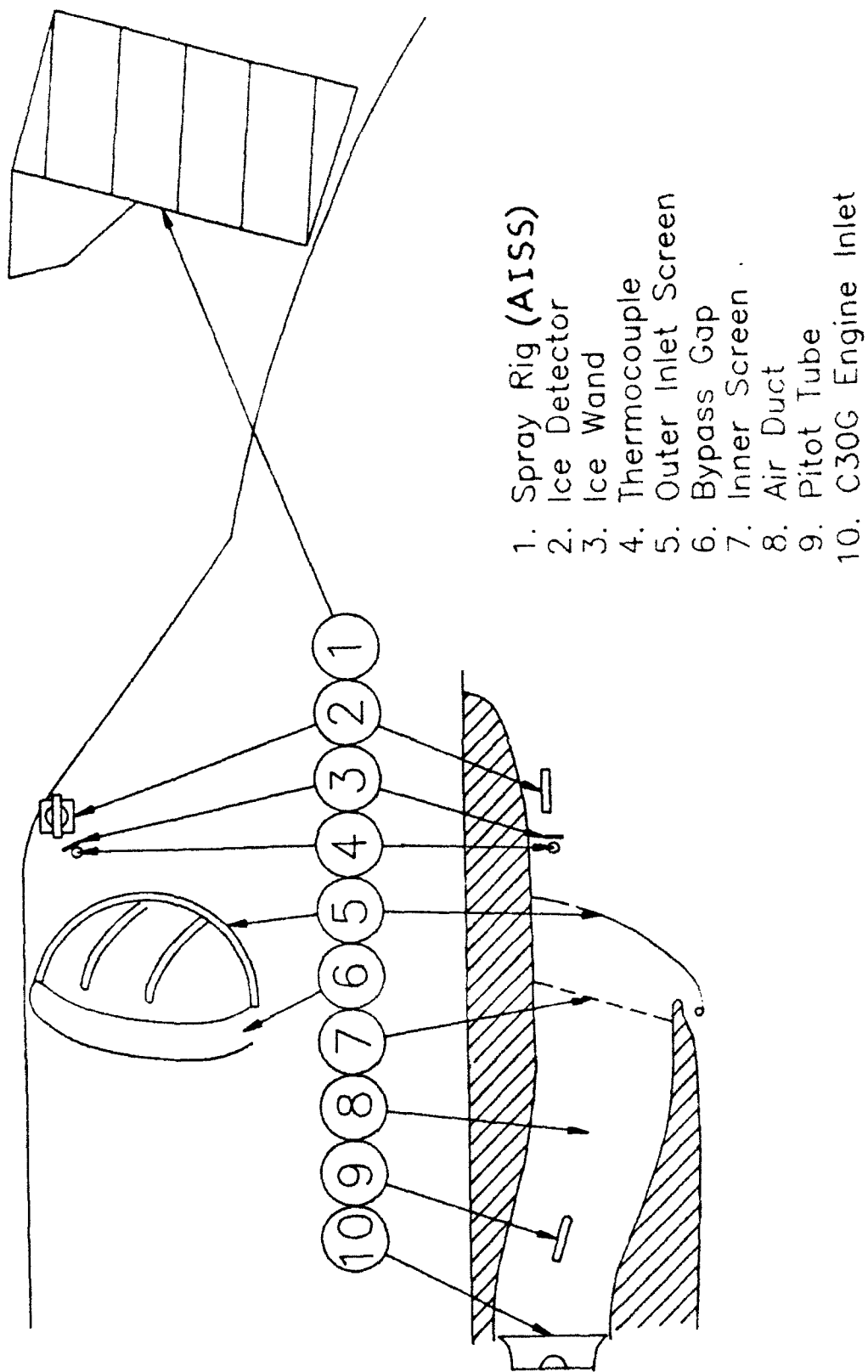


Figure 12. Test Aircraft Configuration
and Set Up (Schematic)

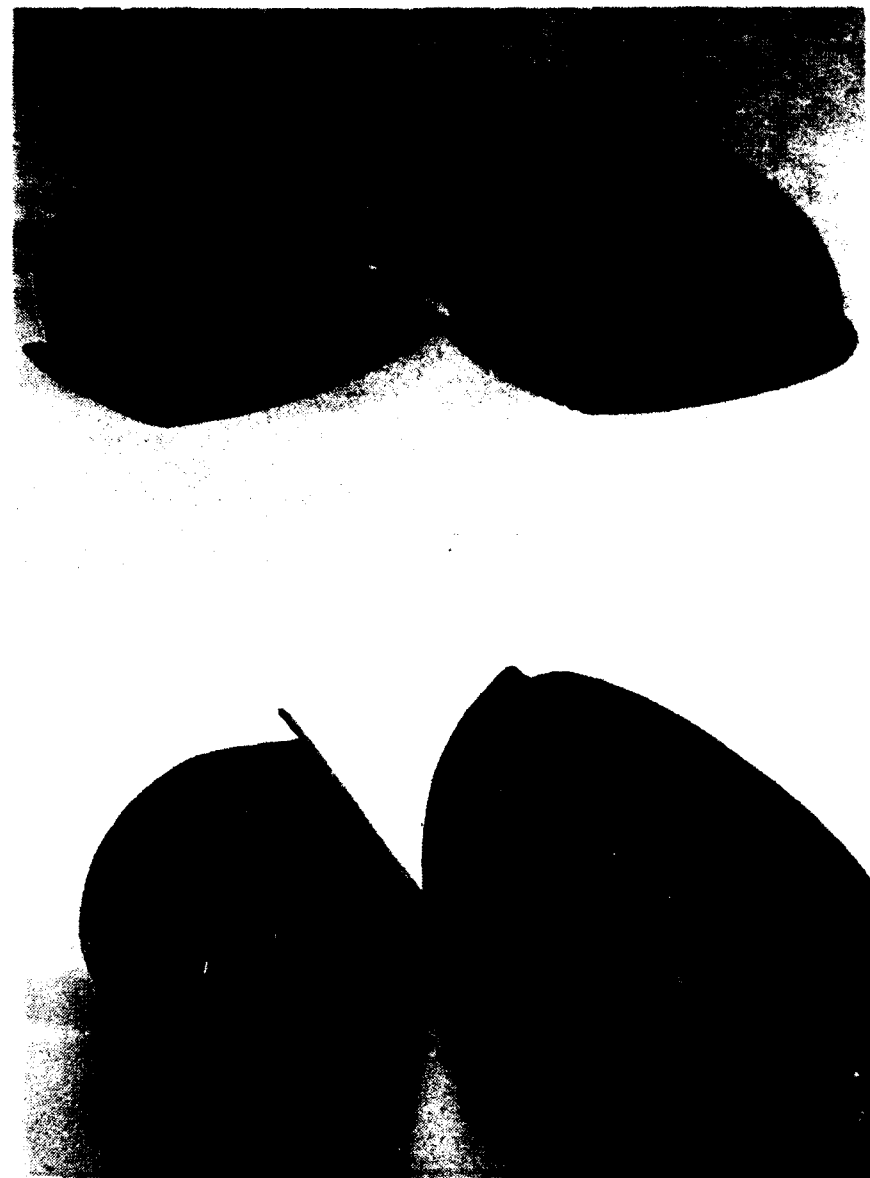


Figure 13. Inlet Screens

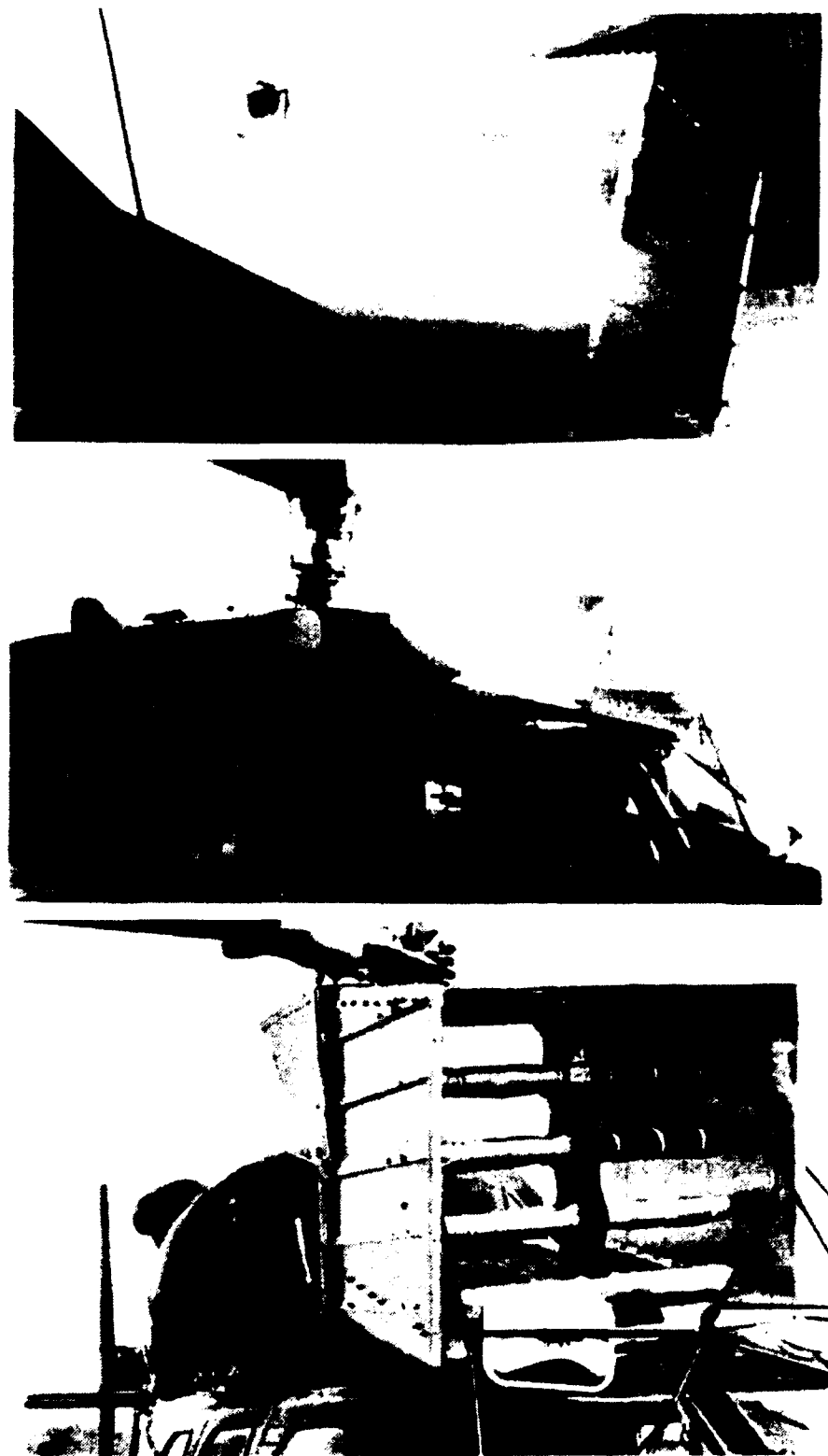


Figure 14. Test Aircraft Configuration Photos.
(Spray Rig)

5B

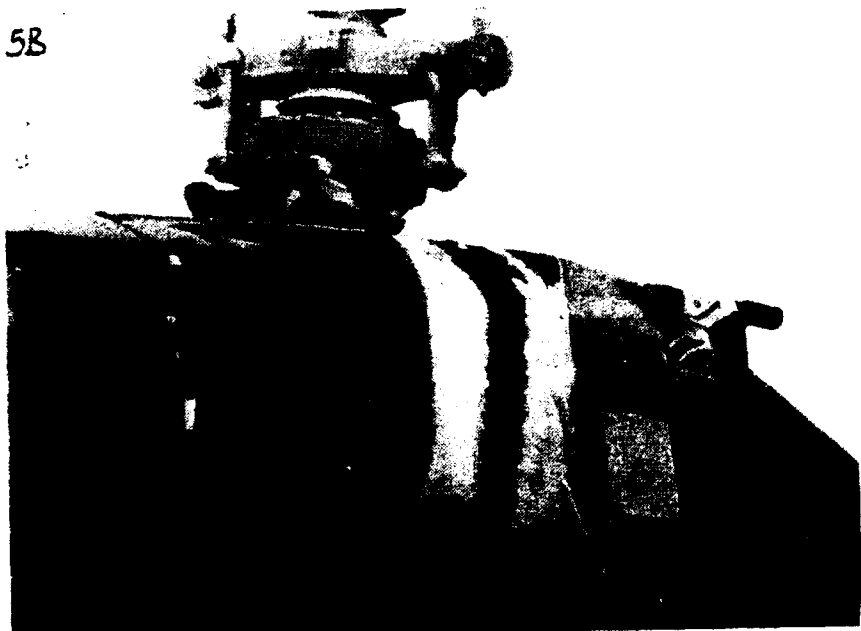


Figure 15. Test Aircraft Configuration Photos.
(Engine Inlet)

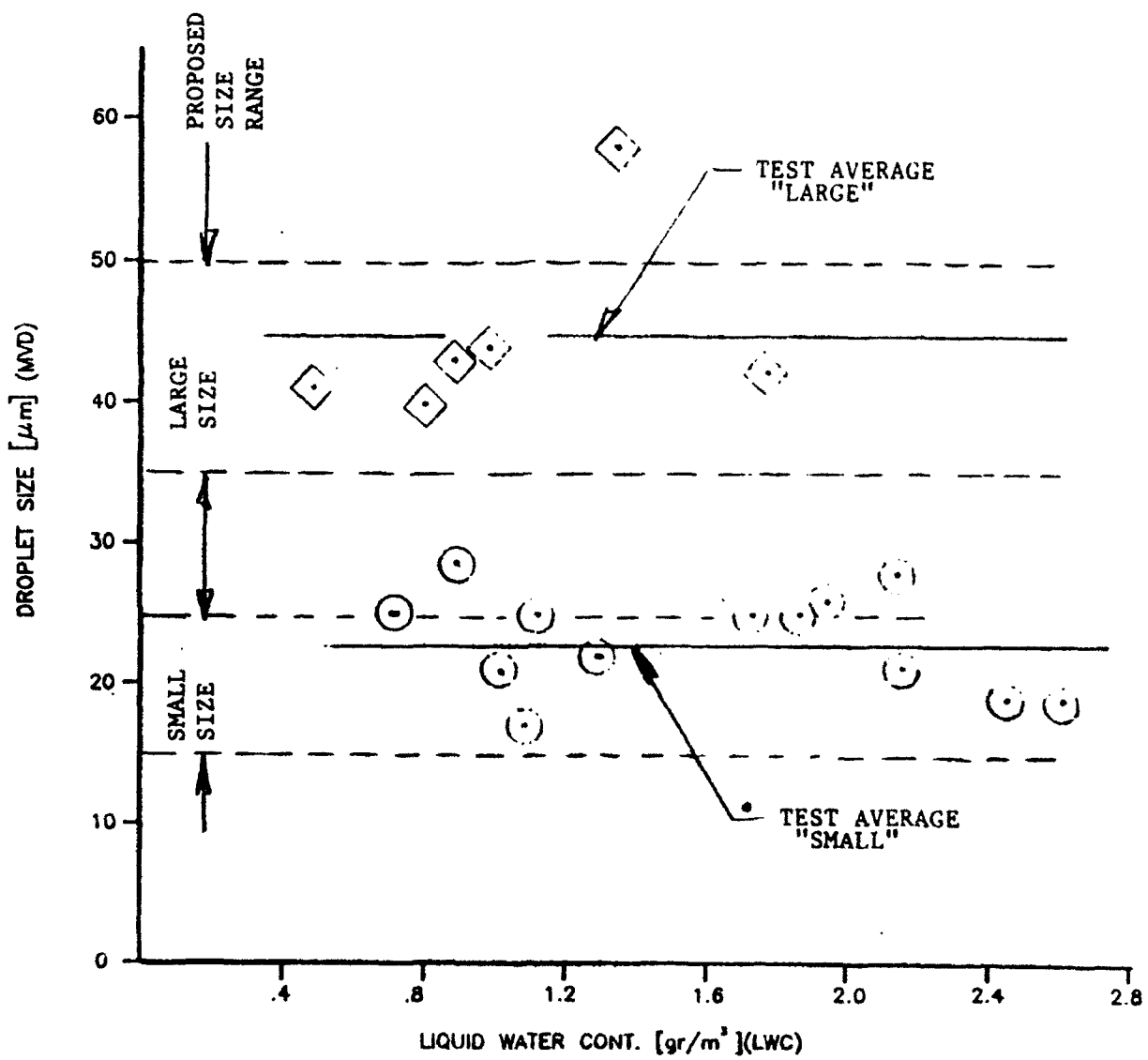


Figure 16. Actual Rake Performance

SYM	FRAME	MVD	LWC
O	FRAME #1	19 μm	2.6
□	FRAME #2	22 μm	1.3
◊	FRAME #3	25 μm	.7
▽	FRAME #4	28 μm	2.1
▼	FRAME #5	21 μm	1.0
○	FRAME #10	26 μm	1.9
○	FRAME #11	25 μm	1.1
○	FRAME #12	25 μm	1.9
○	FRAME #14	21 μm	2.2
+	FRAME #15	17 μm	1.1
+	FRAME #16	20 μm	2.5
x	FRAME #17	26 μm	.71

STRATIFORM CLOUD
NOMINAL BASE LINE
MVD = 21
LWC = .60 gr/m³

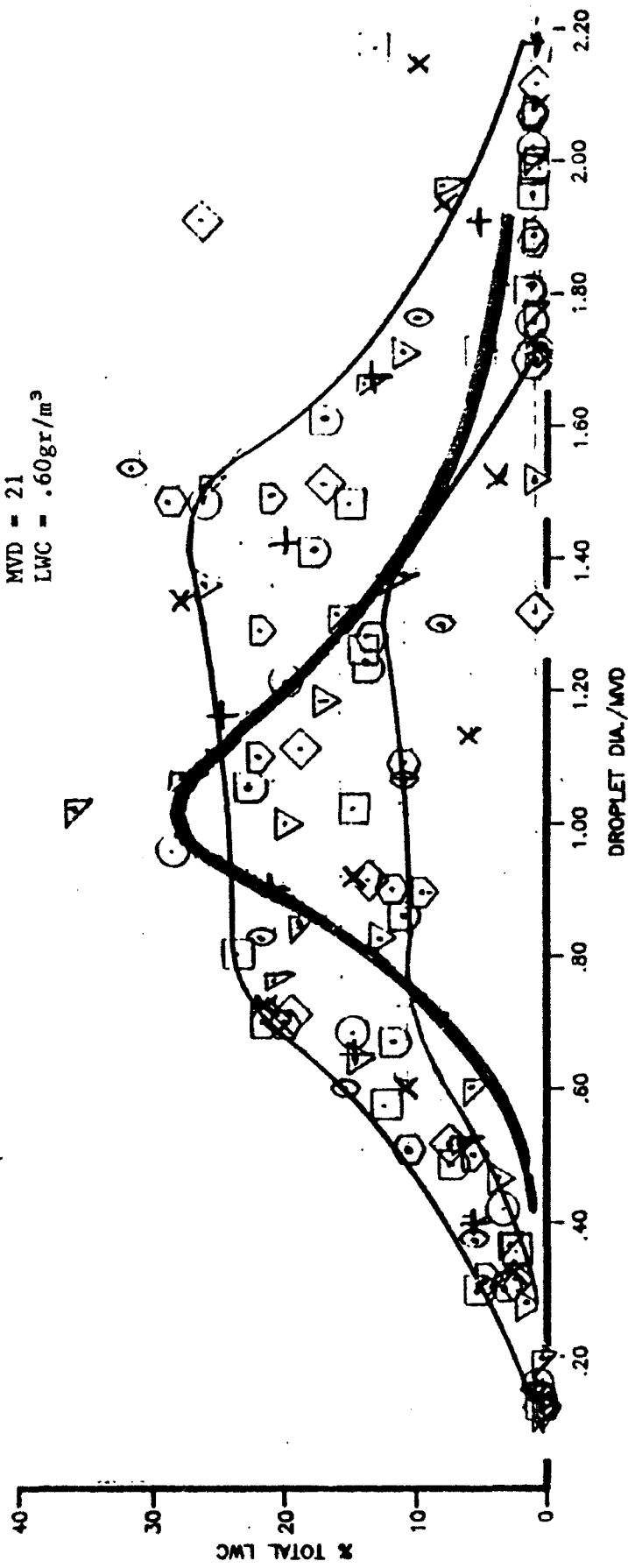


Figure 17. Droplet Size Distribution

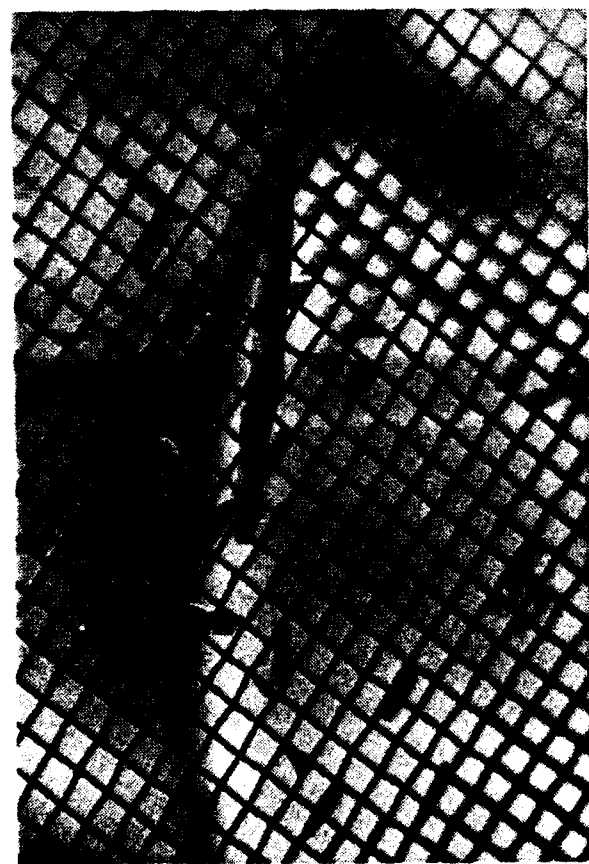


Figure 18. RUN 5A, Maximum Inlet Ice Build Up. Figure 19. RUN 5B, Maximum Inlet Ice Build Up.
MVD = 16, KIAS = 50, OAI = 17°F
MVD = 26, KIAS = 50, OAI = 15°F



Figure 20. RUN 5D, Maximum Inlet Ice Build Up.
MVD - 21, KIAS = 75, DAI = 16°F
Figure 21. RUN 5D, Maximum Inlet Ice Build Up.
MVD - 40, KIAS = 100, DAI = 19°F

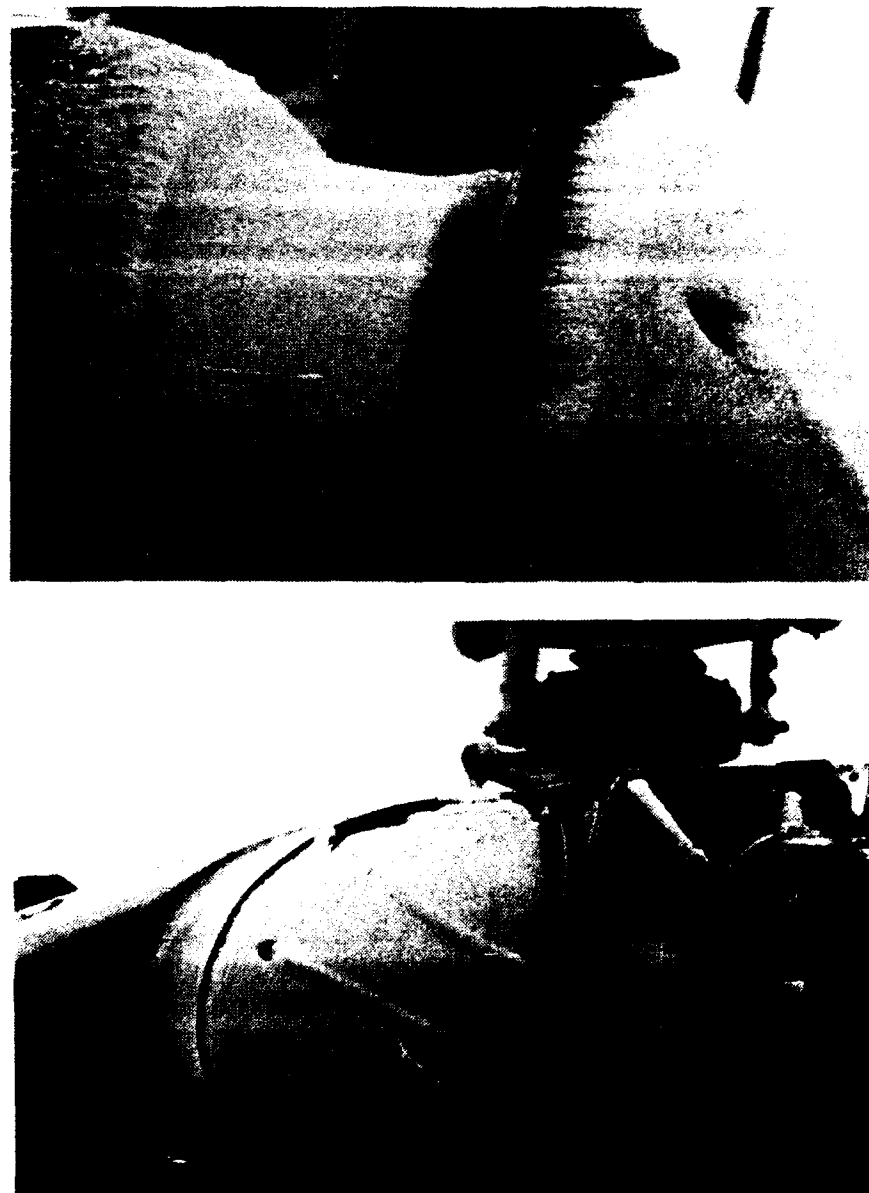


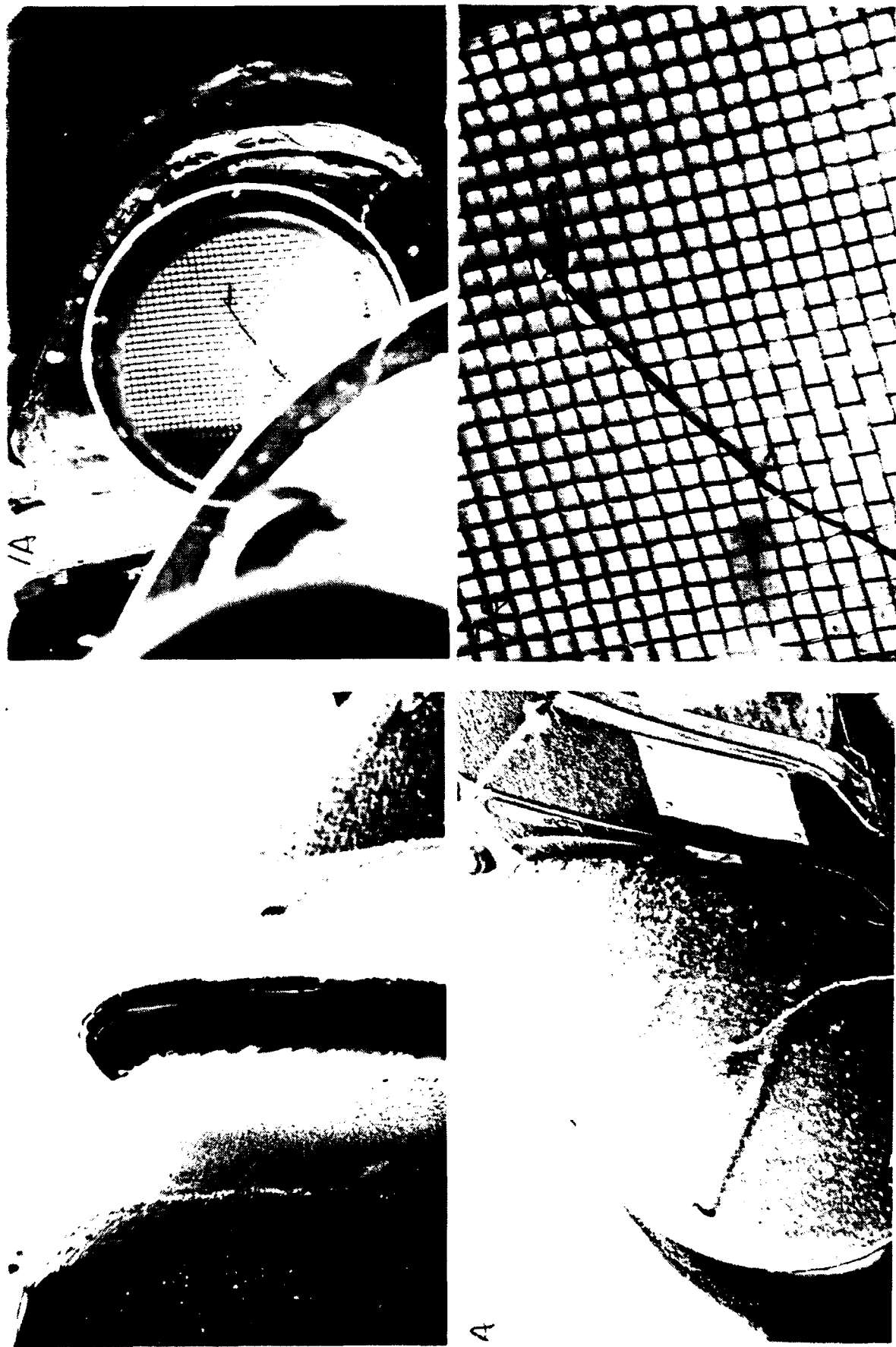
Figure 22. RUN 5E, Maximum Inlet Ice Build Up.
MVD = 58, KIAS = 50, DAT = 17°F



Figure 23. RUN 6A, Maximum Inlet Ice Build Up.
MVD = 26, KIAS = 50, OAT = 11°F

Figure 24. RUN 6B, Maximum Inlet Ice Build Up.
MVD = 25, KIAS = 50, OAT = 14°F

Figure 25. Run 7A, Maximum Inlet Line Blockage.
10, KIAS = 50, OAI = 41



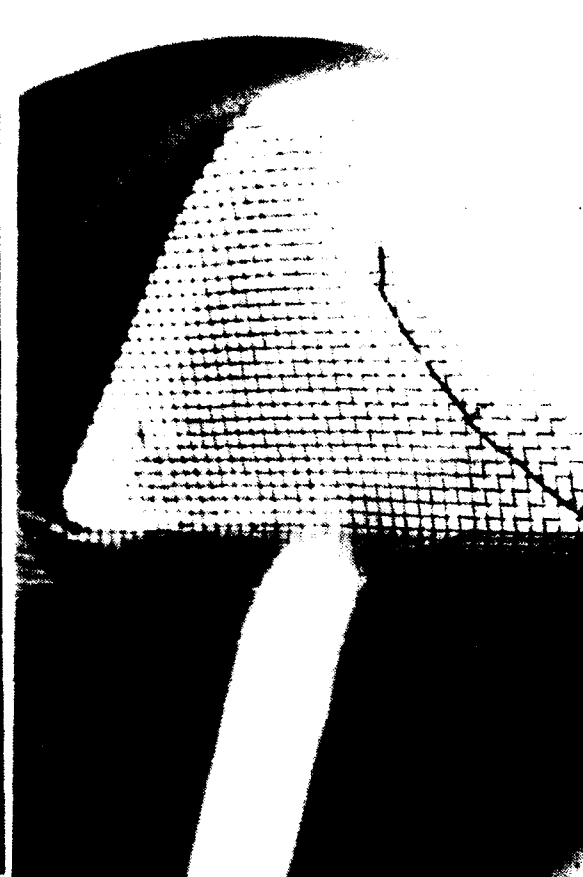


Figure 26. RUN 7B, Maximum Inlet Ice Build Up. Figure 27. RUN 8A, Maximum Inlet Ice Build Up.
MVD = 25, KIAS = 100, DAT = -2°F MVD = 43, GROUND RUN, OAI = 24°F

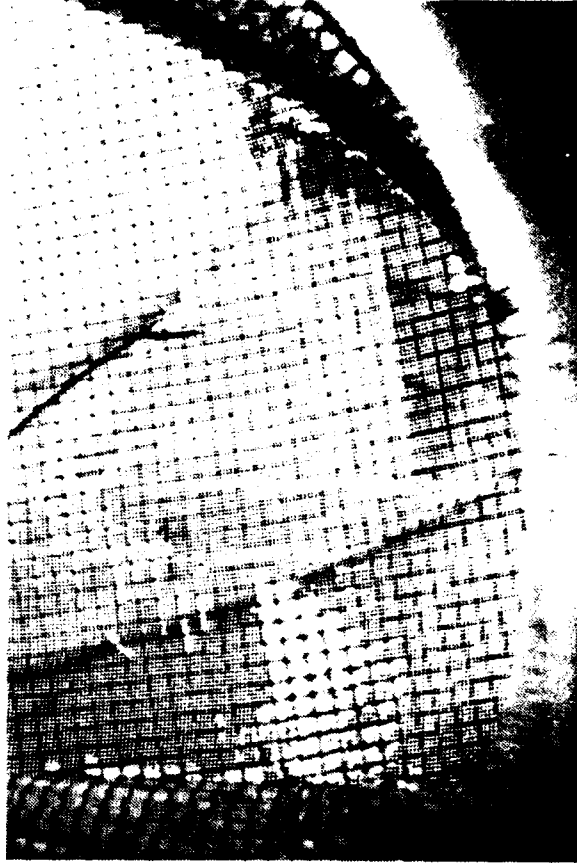
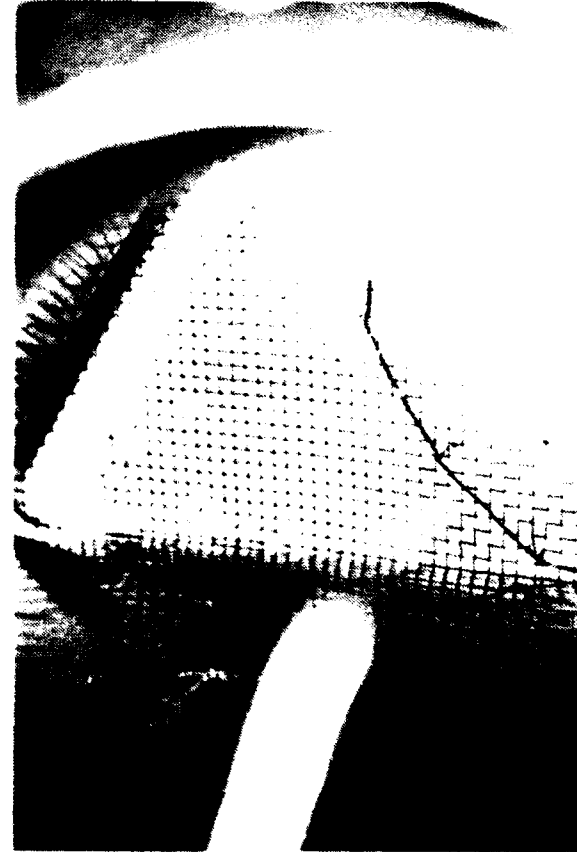


Figure 28. RUN 9A, Maximum Inlet ice build up. Figure 29. RUN 9B, Maximum Inlet ice build up.
MVD = N.A., GROUND RUN, OAI = 52°F , HWD = 50°F , T_{in} = 50°F , T_{out} = 51°F .